Summer 1992 THESIS

The Effects of Atmospheric Constituents on the Normalized Difference Vegetation Index in West Africa

Captain Matthew R. Williams

AFIT Student Attending: Florida State University AFIT/CI/CIA-92-117

AFIT/CI
Wright-Patterson AFB OH 45433-6583

THE EFFECTS OF ATMOSPHERIC CONSTITUENTS ON THE NORMALIZED DIFFERENCE VEGETATION INDEX IN WEST AFRICA

Name: Matthew Redmond Williams
Rank: Captain
Service Branch: USAF
Number of pages: 99
Degree: M.S.
Term Degree Awarded: Summer, 1992
Institution: Florida State University

This paper presents the results of a study of the effects of atmospheric water vapor and aerosols on the Normalized Difference Vegetation Index (NDVI) in West Africa and the corrections of NDVI for these effects. Spatio-temporal patterns of water vapor, aerosols and the secondary NDVI maximum outside the growing season are described. Relationships between NDVI and water vapor were described using linear correlations. Corrections for water vapor and aerosols were done using linear and log-linear regression. NDVI-rainfall correlations were calculated for both corrected and uncorrected NDVI data.

The secondary NDVI peak showed definite spatio-temporal patterns, with clustered peaks in some years and more widespread distributions in other years. Linear correlations between NDVI and water vapor anomalies revealed inverse relationships in the transition to the wet season with little or no correlation at other times of the year. Correlations between running means of NDVI and water vapor showed an out of phase relationship in most cases.

Corrections of NDVI for water vapor reduced the secondary NDVI peak in most cases. The corrections caused an increase in annually integrated NDVI which was most pronounced in dry regions. Aerosol corrections also reduced the secondary peak for the majority of cases.

Water vapor corrected NDVI-rainfall correlations were not found to be statistically significantly better than uncorrected NDVI-rainfall correlations. A relationship between the phase and amplitude of NDVI, rainfall and water vapor was noticed.

Future studies involving atmospheric corrections of NDVI should use the same dates for NDVI, water vapor and aerosol data. This would eliminate data inconsistencies found in this study.

THE FLORIDA STATE UNIVERSITY

COLLEGE OF ARTS AND SCIENCES

THE EFFECTS OF ATMOSPHERICS CONSTITUENTS ON THE NORMALIZED DIFFERENCE VEGETATION INDEX IN WEST AFRICA

By

MATTHEW REDMOND WILLIAMS

A Thesis submitted to the
Department of Meteorology
in partial fulfillment of the
requirements for the degree of
Master of Science

Degree Awarded:

Summer Semester, 1992

The members of the Committee approve the thesis of Matthew Redmond Williams defended on June 26, 1992.

Sharon E. Nicholson
Professor Directing Thesis

Eric A. Smith
Committee Member

Kevin A. Kloesel
Committee Member

Acknowledgments

I would like to express my thanks to my major professor, Dr. Sharon E. Nicholson, for all her support and and guidance during my research. I would also like to thank my committee members, Dr. Eric A. Smith and Dr. Kevin A. Kloesol for their help and advice. In addition, I would like to thank the US Air Force for providing me a chance to attend graduate school.

My thanks also go to the rest of the inmates in the zoo (room 303A): Andrew Lare, Ian Palao and Hanzhi Zheng. Your company and support as well as ridiculous topics of discussion are deeply appreciated. Special thanks go to Jeeyoung Kim for helping me exorcise the demons in my programs and to Andrew Lare (I hear those planes a'tiltin') for answering my questions on anything and everything.

Finally, but most important, I thank my wife, Hwa Il, for all her love and understanding. Without her, I could never have come this far.

Contents

List of Tables

List of Figures

Abstract

This paper presents the results of a study of the effects of atmospheric water vapor and aerosols on the Normalized Difference Vegetation Index (NDVI) in West Africa and the corrections of NDVI for these effects. Spatio-temporal patterns of water vapor, aerosols and the secondary NDVI maximum outside the growing season are described. Relationships between NDVI and water vapor were described using linear correlations. Corrections for water vapor and aerosols were done using linear and log-linear regression. NDVI-rainfall correlations were calculated for both corrected and uncorrected NDVI data.

The secondary NDVI peak showed definite spatio-temporal patterns, with clustered peaks in some years and more widespread distributions in other years. Linear correlations between NDVI and water vapor anomalies revealed inverse relationships in the transition to the wet season with little or no correlation at other times of the year. Correlations between running means of NDVI and water vapor showed an out of phase relationship in most cases.

Corrections of NDVI for water vapor reduced the secondary NDVI peak in most cases. The corrections caused an increase in annually integrated NDVI which was most pronounced in dry regions. Aerosol corrections also reduced the secondary peak for the majority of cases.

Water vapor corrected NDVI-rainfall correlations were not found to be statistically significantly better than uncorrected NDVI-rainfall correlations. A relationship between the phase and amplitude of NDVI, rainfall and water vapor was noticed.

Future studies involving atmospheric corrections of NDVI should use the same dates for NDVI, water vapor and aerosol data. This would eliminate data inconsistencies found in this study.

Chapter 1

Introduction

The Sahel, an area of West Africa on the southern border of the Sahara, is subject to severe and extended droughts. Drought conditions have existed over West Africa for the last two decades (Nicholson 1989). The combined effects of drought and human activities, such as overgrazing, can adversely effect the Sahelian vegetation.

In recent years, an attempt to monitor vegetation through satellite techniques has been developed. The National Oceanic and Atmospheric Administration (NOAA) satellites (e.g. NOAA 7-9) carry the Advanced Very High Resolution Radiometer (AVHRR), which can provide visible and infrared reflectance data. The photosynthetic process allows for the use of this reflectance data to monitor plant growth. To understand how remote sensing of vegetation is possible, it is useful to understand how plants "work". The photosynthetic process in plants is driven by photosynthetically active radiation (PAR)(0.4-0.7μm) in the following reaction:

$$CO_2 + H_2O \Rightarrow lightenergy \Rightarrow CH_2O + O_2. \quad (1)$$

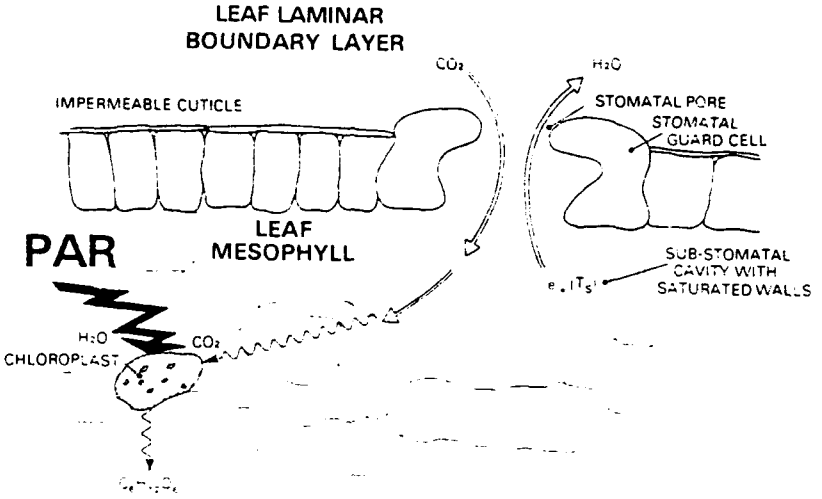

Figure 1: The process of photosynthesis (from Tucker and Sellers, 1986)

This reaction takes place in plant organelles called chloroplasts (Figure 1). Only 2-3% of PAR is reflected toward space, the rest is transmitted or absorbed (Tucker and Sellers 1986). The PAR is absorbed within green leaves by chlorophylls A and B and carotenoids. Spectrally, high absorption of incident radiation occurs from 0.4-0.7μm, lower absorption from 0.7-1.3μm and high absorption again from 1.3-2.5μm. The first band is related to plant pigments present, the second to projected green-leaf density and the last to liquid water present. Since the bands related to plant pigments (0.4-0.7μm) and liquid water content (1.3-2.5μm) are highly coupled, satellites can use the 0.4-0.7μm and .7-1.3μm bands for reflectance measurements.

Tucker *et al.* (1983, 1985a, 1985b) developed the Normalized Difference Vegetation Index (NDVI) using channels 1 and 2 on the NOAA series satellites. Channel 1 covers 0.58-0.68μm

and channel 2 covers 0.725-1.1μm. NDVI is then defined as:

$$NDVI = \frac{c_2 - c_1}{c_2 + c_1} \tag{2}$$

where c_1 is channel 1 and c_2 is channel 2. NDVI is restricted to values between -1.0 and 1.0. Table 1 shows values of NDVI for various degrees of vegetation as well as bare soil, clouds, snow, ice, and water. NDVI has been related to various vegetation parameters such as net primary production, total dry matter accumulation and vegetation phenology (Tucker and Sellers 1986, Tucker *et al.* 1983, Justice *et al.* 1985).

Table 1: Stratification of the NDVI response to broad scene components as measured from NOAA-7 (From Holben 1986).

	Planetary Albedo		
Cover type	Channel 1	Channel 2	NDVI
Dense green-leaf vegetation	0.050	0.150	0.500
Medium green-leaf vegetation	0.080	0.110	0.140
Light green-leaf vegetation	0.100	0.120	0.090
Bare soil	0.269	0.283	0.025
Clouds (opaque)	0.227	0.228	0.002
Snow and ice	0.375	0.342	-0.046
Water	0.022	0.013	-0.257

There are some important influences on the value of NDVI besides vegetation. Viewing angle, illumination geometry, background soil and atmospheric effects alter the value of NDVI. Table 2 lists these various effects on the two channels and how those effects alter the NDVI. The viewing angle of the vegetation by the sensor varies as the sensor scans the scene. As it scans from the backscatter direction to forward scatter, the viewing angle changes $\pm$ 54° from nadir. Off nadir viewing tends to decrease NDVI, since the reflectances must travel through more of the atmosphere. This can lead to a decrease of the NDVI by

approximately 0.10 NDVI units (Holben 1986). The illumination geometry also changes as the solar zenith angle varies by 20° across a scan and by 47° due to seasonal changes for 30° latitude. This produces a decrease in NDIV of about 0.01 units for near nadir viewing angles and close to 0.1 units for off nadir viewing angles between the winter and summer solstice (Holben 1986). These results are due to shadowing effects of the changing solar zenith angles.

Table 2: Factors influencing the value of NDVI.

Factor	Channel 1	Channel 2	NDVI
Aerosols	Decrease/ increase	Decrease/ Increase	Generally decrease
Water vapor	Decrease	Little effect	Decrease
Rayleigh scattering	Generally invariant, little effect		
Oxygen	Decrease	Little effect	Decrease
Ozone	Little effect	Decrease	Increase
Viewing angle	Decrease	Decrease	Decrease
Illumination	Decrease	Decrease	Decrease
Soil: wet	Decrease	Decrease	Decrease
Soil: dry	Increase	Increase	Increase
Soil: 75% or less cover	Increase	Little effect	Increases
Cloud contamination	Decrease	Increase	Decrease

In semi-arid and arid regions, such as the one in this study, the surface soil also influences the NDVI. Huete *et al.* (1985) found that NDVI is independent of background soil only with 75% or greater areal coverage of plants. They showed that soil moisture also affects NDVI, and these effects are strongest for vegetation cover of less than 75%. For a 40% vegetation cover, a moist soil could have an increased NDVI of nearly 0.1 NDVI units. This is due to more of the near-infrared (NIR) radiation being transmitted through vegetation, while the

red light is absorbed.

Atmospheric constituents, such as air molecules, water vapor and aerosols, also affect NDVI. Rayleigh scattering is nearly invariant over time and the change in NDVI due to Rayleigh scattering would also be small. Oxygen absorbtion would tend to decrease the NIR and decrease the NDVI. These decreases would be less than one percent (Holben 1986). Water vapor decreases the response in the near-infrared (NIR) channel. This decreases the value of NDVI by up to 0.1 NDVI units for a water vapor content of 8 g/cm^2 and a nadir viewing angle (Justice *et al.* 1991). Aerosols also decrease the NDVI signal due to both absorption and scattering. Holben *et al.* (1991) has shown a decrease of 0.02 NDVI units for an increase of aerosol optical thickness of 1.0.

Cloud contamination is also a problem. Holben (1986) describes a technique called maximum value compositing (MVC). The technique involves a seven day composite using a thermal cloud mask. The compositing technique selects, on a pixel by pixel basis, the maximum value of NDVI for the seven day period. The thermal cloud mask sets a threshold of 285K brightness temperature on AVHRR channel 5 (10.5-11.5μm). It is assumed that the African landmass would have a temperature above this threshold, thus any pixels which are less than the threshold are set to zero. A similar approach is taken in the visible channel (.62-.72μm), with reflectances above a threshold being set to zero.

Holben's 1986 study demonstrated that MVC tends to select NDVI from near nadir and with small solar zenith angles. In addition, water vapor and aerosol effects are reduced; however, these effects are not eliminated.

Recently, studies have been made relating NDVI to rainfall variability (Malo and Nicholson 1990; Nicholson *et al.* 1990; Davenport and Nicholson 1991). In their study of NDVI-rainfall relationships for Sahelian West Africa, Malo and Nicholson noted "anomalous" peaks in the NDVI signal outside of the growing season. They speculated that the secondary peaks were caused by changes in water vapor and aerosol concentrations. These peaks suggest that the NDVI signal is being altered by the influences described in Table 2. As mentioned, the maximum value compositing technique of Holben tends to offset the effects of many of these factors. Huete and Tucker (1991) have stated that atmospheric water vapor differences between wet and dry seasons exceed variations caused by secondary soil influences. Cloud contamination effects tend to be stronger along coastal regions of West Africa and less pronounced in the interior (Eck and Kalb 1991). Correcting NDVI for the effects of atmospheric water vapor and aerosols may reduce or eliminate the anomalous secondary peaks. It may as well lead to improved estimates of primary production.

The purpose of this study then, is to: examine the spatial and temporal patterns of water vapor, aerosols and the secondary peak in the NDVI signal; examine relationships between NDVI and water vapor; "correct" the NDVI for the effects of water vapor and aerosols in an attempt to reduce the magnitude of the secondary peak; and to examine the effect of corrections on annually integrated NDVI and NDVI-rainfall correlations.

The spatial and temporal patterns of the secondary peak will be shown using a "vector" representing the magnitude and phase of the peak. Contoured maps will be used to present the water vapor patterns and time series will be used for the aerosols. The relationship between NDVI and water vapor will be shown using a linear correlation. Water vapor

corrections to NDVI will be made using a regression equation (Ben Mohamed and Frangi 1983) regressing precipitable water from water vapor. Corrections for aerosols will be made using a linear regression of reflectance data calculated from radiative transfer models in Justice *et al.* (1991) and Holben *et al.* (1991). Rainfall-NDVI correlations will be made using lagged linear correlations.

1.1 Geography and Climatology of West Africa

This study involves an area of West Africa extending from approximately 10°N to 20°N and from 15°E to 18° W. This includes a large portion of what is called the Sahel, while the Sahara occupies the northern portion of this region. The Saharan portion is comprised mostly of sandy dunes (ergs), rocky desert (hamada) or pebble desert (regs). Two areas of higher terrain are the Adrar des Iforas and the Air (Figure 2), which are southern extensions of the Ahaggar Massif (FAO 1979).

The southern portion of the area, the Sahel, is mostly plains with a few isolated plateaus (Figure 2). The inland delta of the Niger river, where the river expands into a large braided river system, is one exception (FAO 1979).

The vegetation of the area ranges from Sudanian woodland in the south to a transition woodland giving way to a wooded grassland further north, then semidesert grassland and finally desert. In addition, there is an area of largely fresh water swamp and aquatic vegetation which is located around Lake Chad (White 1983).

The climate of West Africa varies, generally, from south to north. Mean temperatures

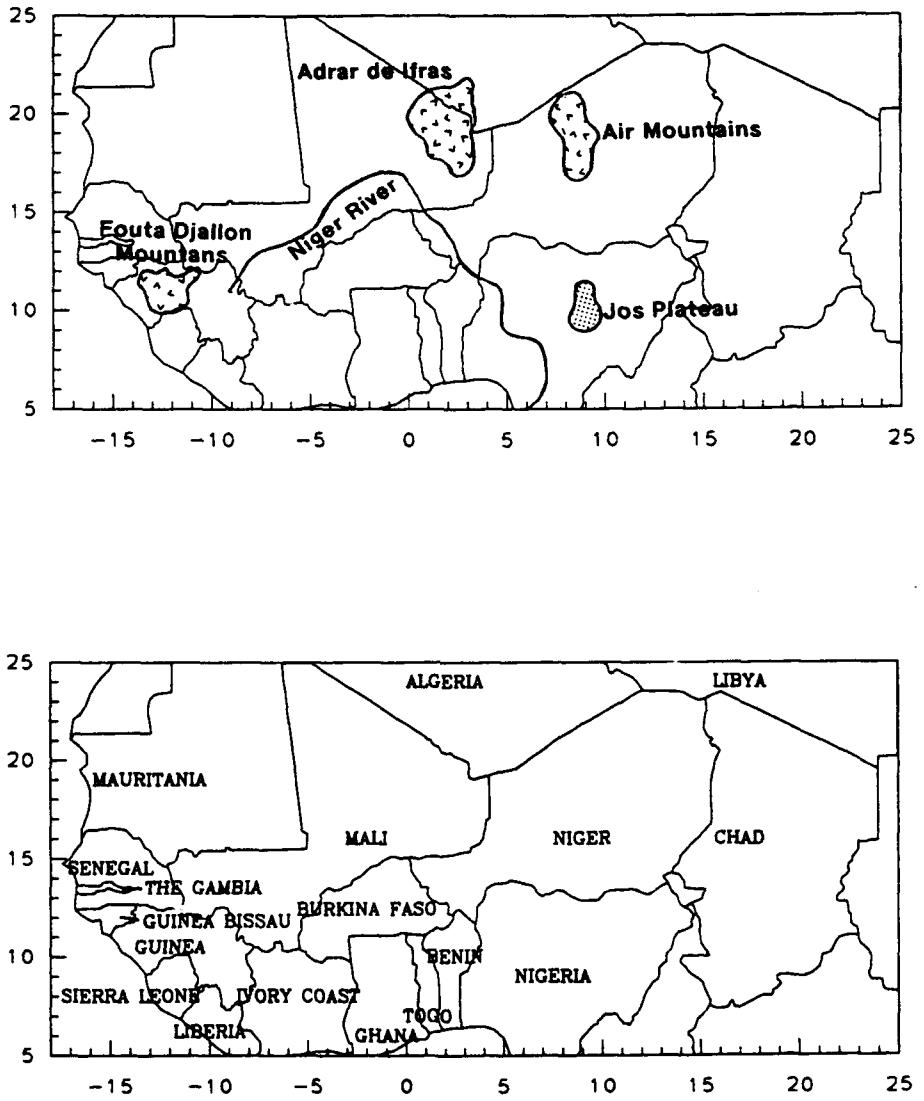

Figure 2: Major geographic features of West Africa (a) and political map of West Africa (b).

in January (Figure 3a.) range from 20°C to 26°C in the north and south, respectively. In August (Figure 3b), the mean temperatures range from 32°C in the north to 26°C in the south (Hayward and Ogutoyinbo 1987).

Pressure and wind patterns in the region are mostly influenced by two systems. These are the subtropical high (or West African Anticyclone) and the Inter-tropical Convergence Zone (ITCZ). From December to February the ITCZ is located between 5°N and 8°N. During this period, most of the area north of the ITCZ (under the influence of the subtropical high) experiences dry northeast winds known as the "harmattan". Blowing or suspended dust is common. From late June to August the ITCZ has moved well north, past 20°N and the southwest monsoon winds predominate over the region. The northeast harmattan can still be found aloft, being undercut by the warmer more moist air of the southwest monsoon (Dubief 1979). The harmattan and dust production will be discussed further in Chapter 3.

Precipitation over the Sahelian region is largely controlled by the movement of mesoscale tropical disturbance lines, moving from east to west, associated with the ITCZ. These lines are most active in the region from June through September. Some of these disturbances are well defined and produce much rain, while others are simply large areas of clouds which produce little or no rain.

Figure 4 shows a plot of annual precipitation in West Africa. Rainfall ranges from more than 1200mm in the south at Bougouni, Mali, to less than 20mm well to the northeast at Bilma, Niger. Most of the Sahel has a unimodal rainfall regime, with maximum rainfall in August. A portion along the Atlantic Coast and some of the northwestern Sahara experience a bimodal rainy season, with maximums in Febrauary and August (Nicholson *et al.* 1988).

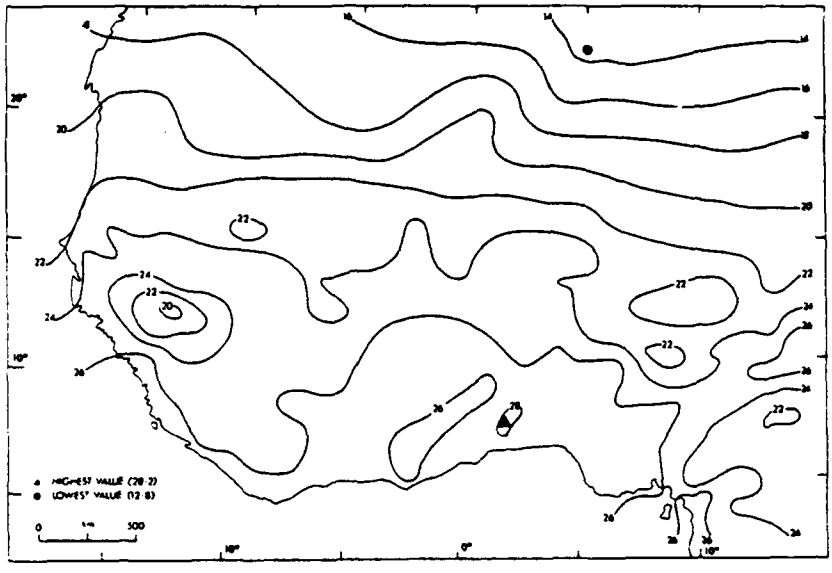

Mean temperatures over West Africa in January

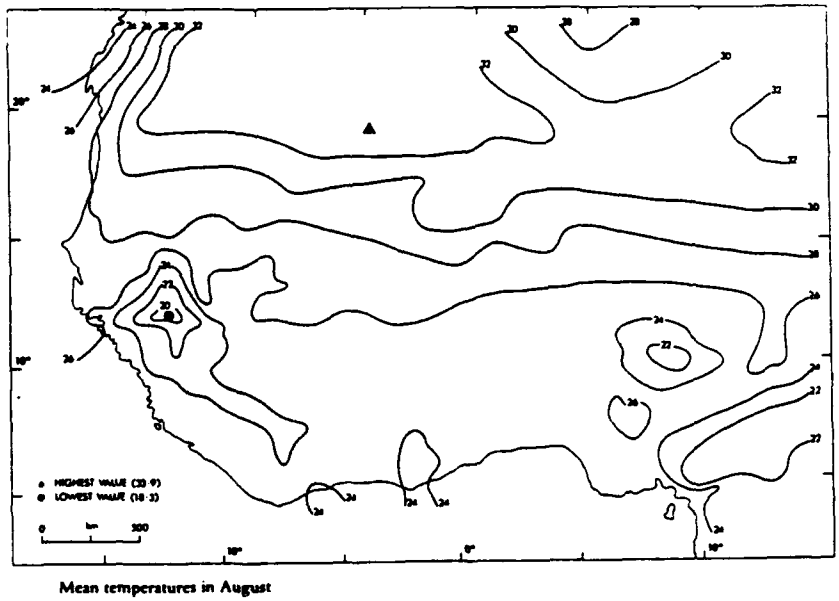

Mean temperatures in August

Figure 3: Mean temperatures for January and August (from Hayward and Ogutoyinbo, 1987).

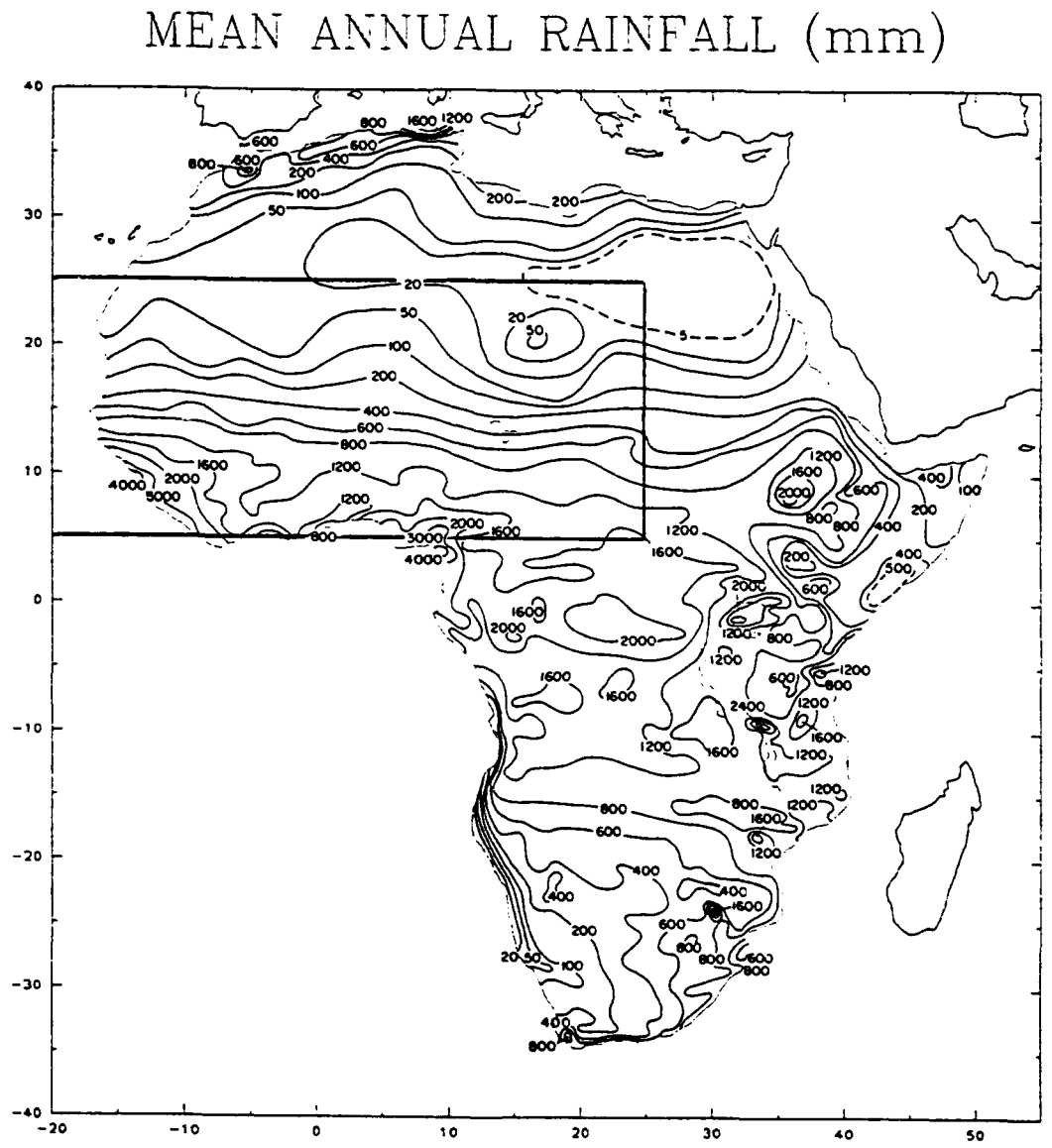

Figure 4: Mean annual preciptation (from Nicholson, 1988). Boxed area is area of interest.

Chapter 2

Data

This study uses monthly composited NDVI, monthly water vapor, aerosol optical thickness, and rainfall data. The period of analysis covers 1982-1988, except for the aerosol analysis. Aerosol optical thickness data was collected from a variety of sources, namely: Cerf (1979); D'Almeida (1987); and Ben Mohamed *et al.* (unpublished manuscript). These studies will be discussed further in Chapter 3.

NDVI data was calculated from NOAA-AVHRR global area coverage (GAC) imagery. The data was provided by Dr. C. J. Tucker of the NASA Goddard Space Flight Center (GFSC). The maximum value compositing technique described in Chapter 1 was used in processing the data. Monthly composites were made by selecting the highest daily value during each compositing period.

Water vapor data was extracted from Monthly Climatic Data for the World (1982-1988). Missing data was replaced with 30 year means. The conversion of water vapor data to precipitable water was done using a regression equation developed by Ben Mohamed and

Frangi (1986) from Sahelian data. The equation is:

$$\ln Pw = 0.47\sqrt{e} - 0.89 \tag{3}$$

where Pw is precipitable water in centimeters and e is observed water vapor pressure in millibars.

Rainfall data were obtained from Dr. Sharon E. Nicholson, Department of Meteorology, Florida State University. This data has been compiled from numerous sources as described in Nicholson *et al.* (1988).

Eighty-one stations were available for determining spatial and temporal patterns of the NDVI peak. Only secondary peaks from 42 of these are displayed on maps for clarity. Twenty seven stations, derived from the original 81, were analyzed for the effects of water vapor. The stations were chosen on the basis of location and availability of water vapor data. In the aerosol related portion of the study, four of the 27, plus three additional stations, were examined. Table 2 shows the list of all stations. Figure 5 shows time series of NDVI, water vapor and rainfall for the 27 stations. There was insufficient rainfall data for Kaolack, Rufisque and St. Louis, Senegal to plot time series.

White's (1983) UNESCO vegetation map of Africa was also used. Vegetation formations were found for each of the 30 stations in the study. Figure 6 shows vegetation formations in the West African region and the location of stations.

It should be noted that although all the data is "monthly", the term monthly does not have the same meaning in each case. In the cases of water vapor and aerosol optical thickness, monthly is the statistical mean of all the daily or twice daily values of those

Table 3: List of 27 Station Names

Kandi, Benin (KAND)	Nema, Mauritania (NEMA)
Bobo Dioulasso, Burkina Faso (BOBO)	Nouakchott, Mauritania (NOUA)
Dori, Burkina Faso (DORI)	Tidjikja, Mauritania (TIDJ)
Fada N'Gourma, Burkina Faso (FADA)	Agadez, Niger (AGAD)
Ouahigouya, Burkina Faso (OUAH)	Bilma, Niger (BILM)
Bamako, Mali (BAMA)	Birni N'Konni, Niger (BIRN)
Bougouni, Mali (BOUG)	Gaya, Niger (GAYA)
Hombori, Mali (HOMB)	N'Guigmi, Niger (NGUI)
Kayes, Mali (KAYE)	Tahoua, Niger (TAHO)
Koutiala, Mali (KOUT)	Tillabery, Niger (TILL)
Aioun El Atrous, Mauritania (AIOU)	Kaolack, Senegal (KAOL)
Akjoujt, Mauritania (AKJO)	Rufisque, Senegal (RUFI)
Atar, Mauritania (ATAR)	St. Louis, Senegal (ST L)
Boutilimit, Mauritania (BOUT)	

Letters in parenthesis correspond to Figure 6

parameters in a individual month. Monthly rainfall is the total accumulation of rainfall in a month. Monthly NDVI, however, is not a mean or an accumulation. It is the maximum value of NDVI selected during the monthly compositing period. It represents reflectances on one specific day for a particular pass of the satellite. The full ramifications of these differences will be discussed further in later chapters.

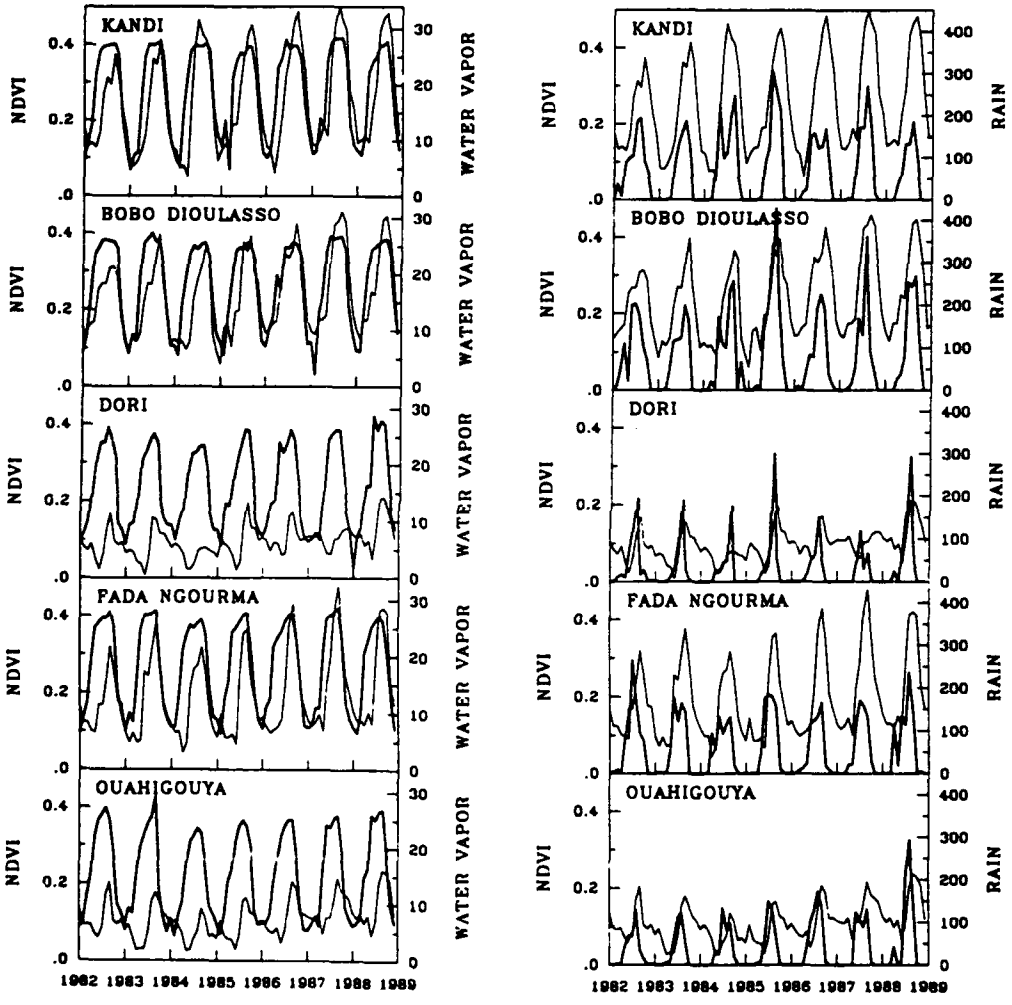

Figure 5: Time series of NDVI, water vapor and rainfall. NDVI is the thin solid line and water vapor and rainfall are thick solid lines.

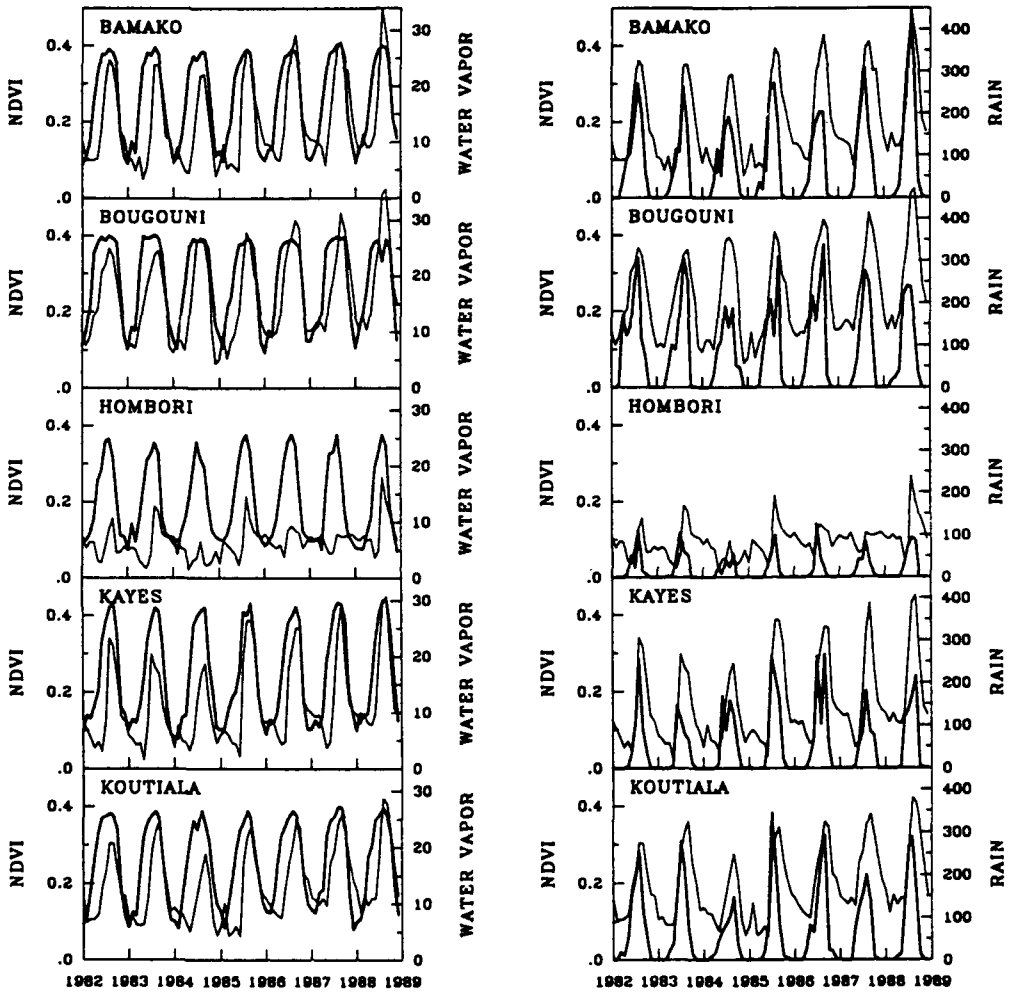

Figure 5: continued.

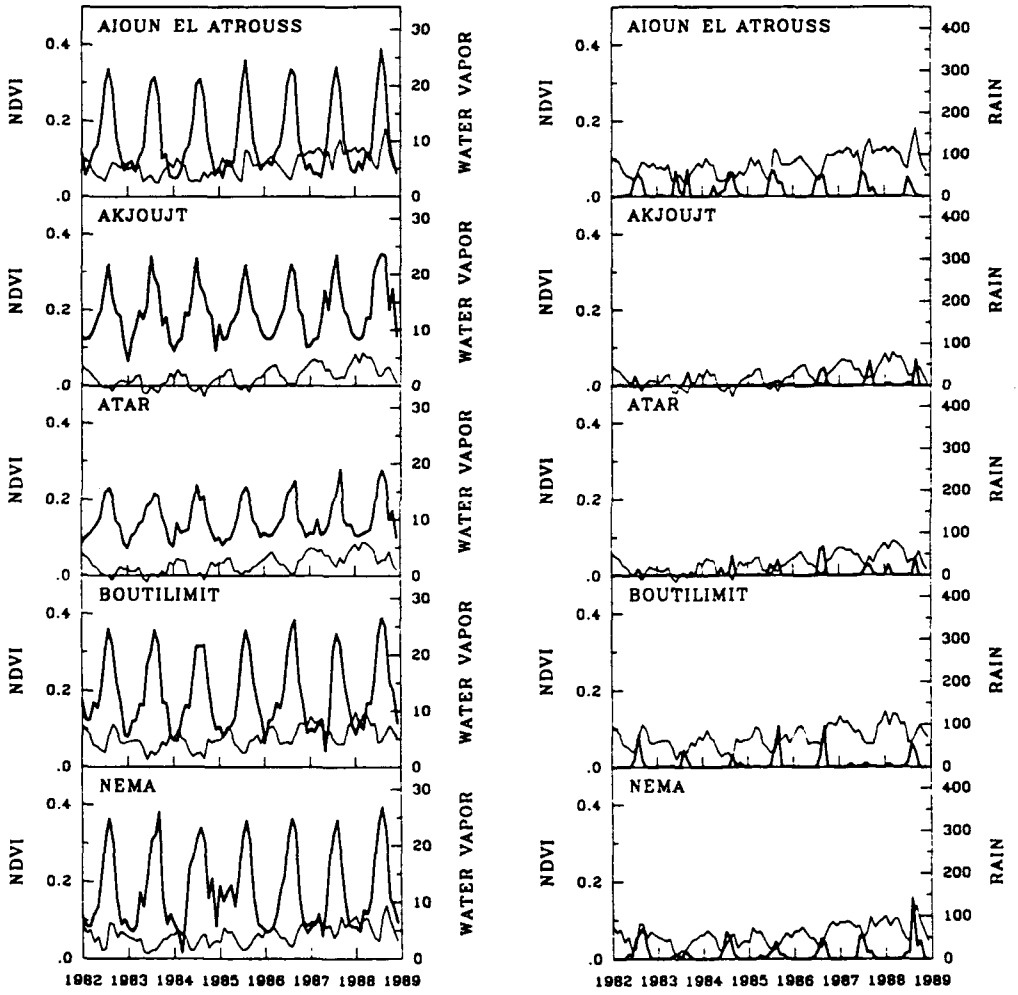

Figure 5: continued.

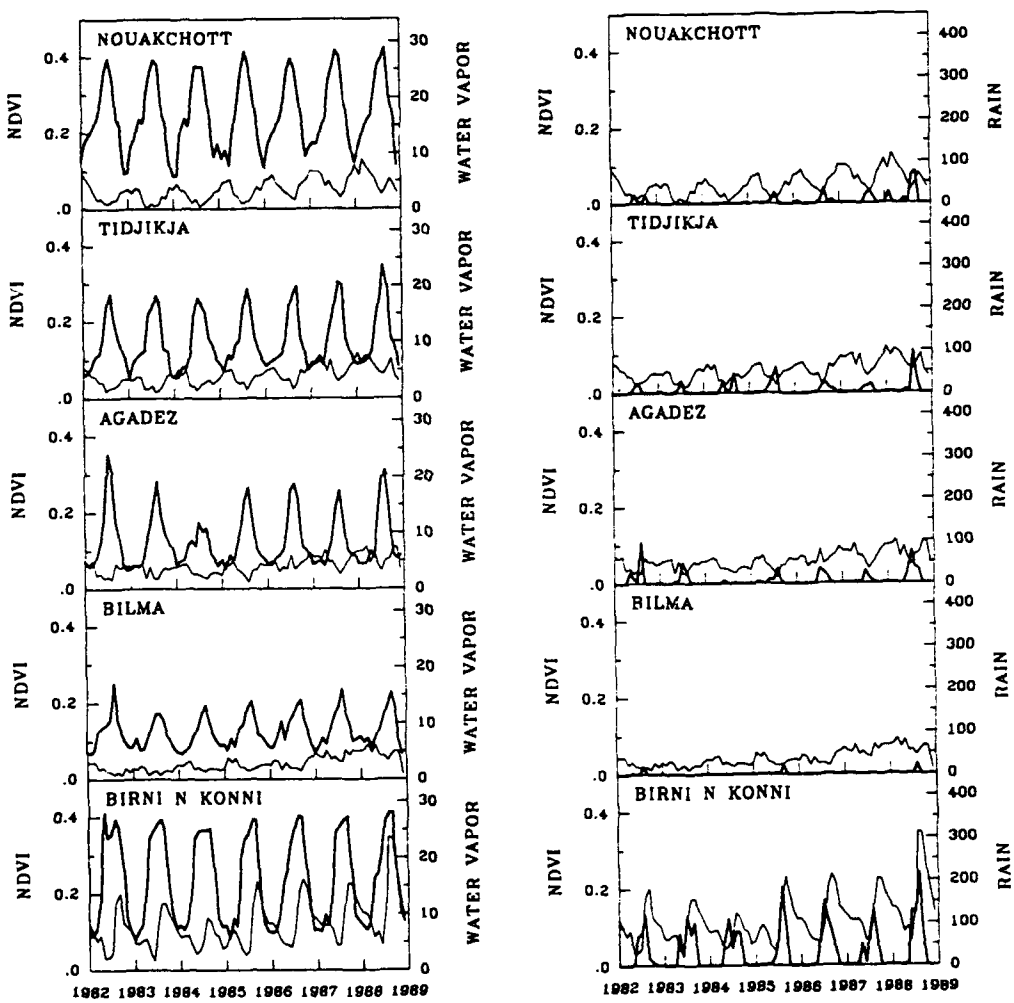

Figure 5: continued.

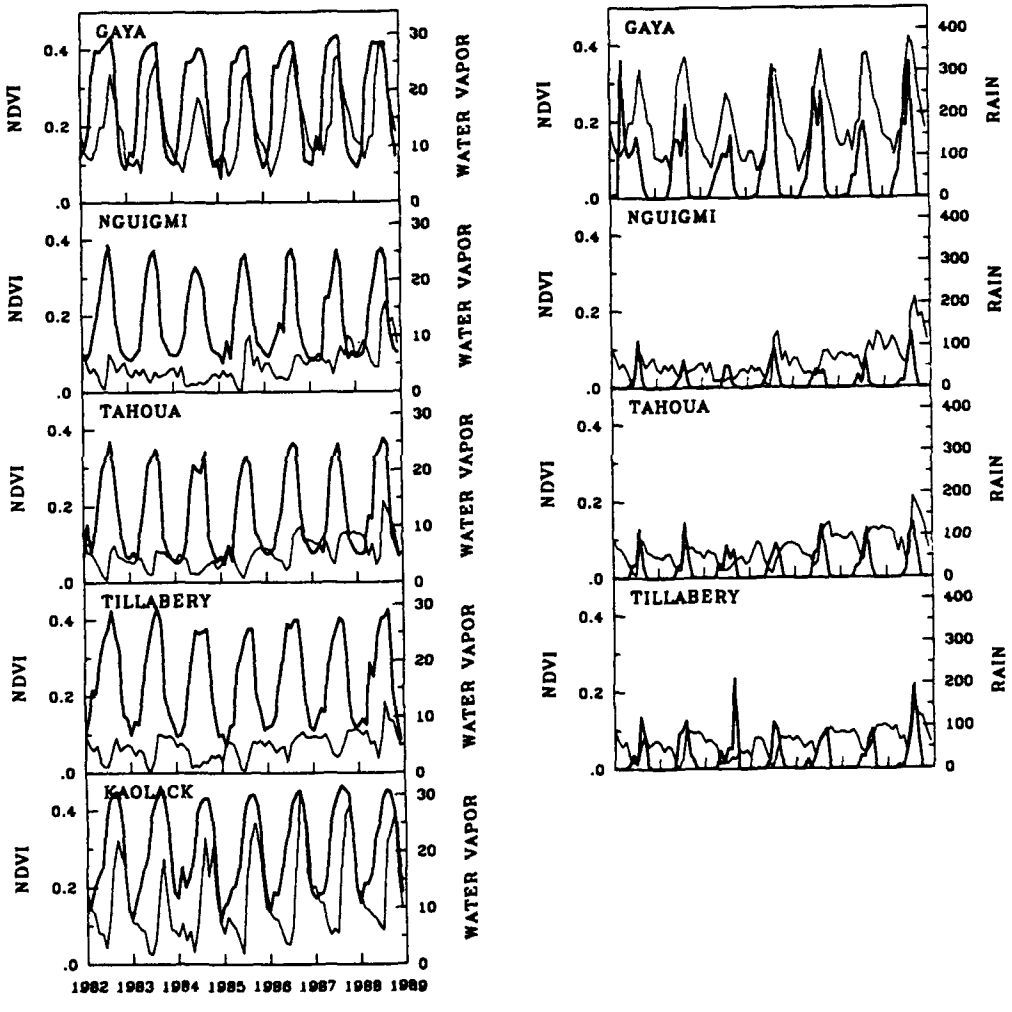

Figure 5: continued.

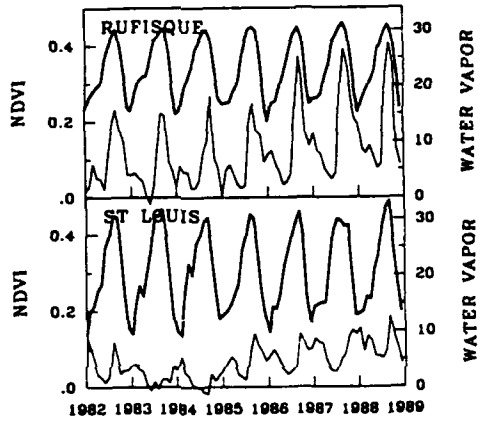

Figure 5: continued.

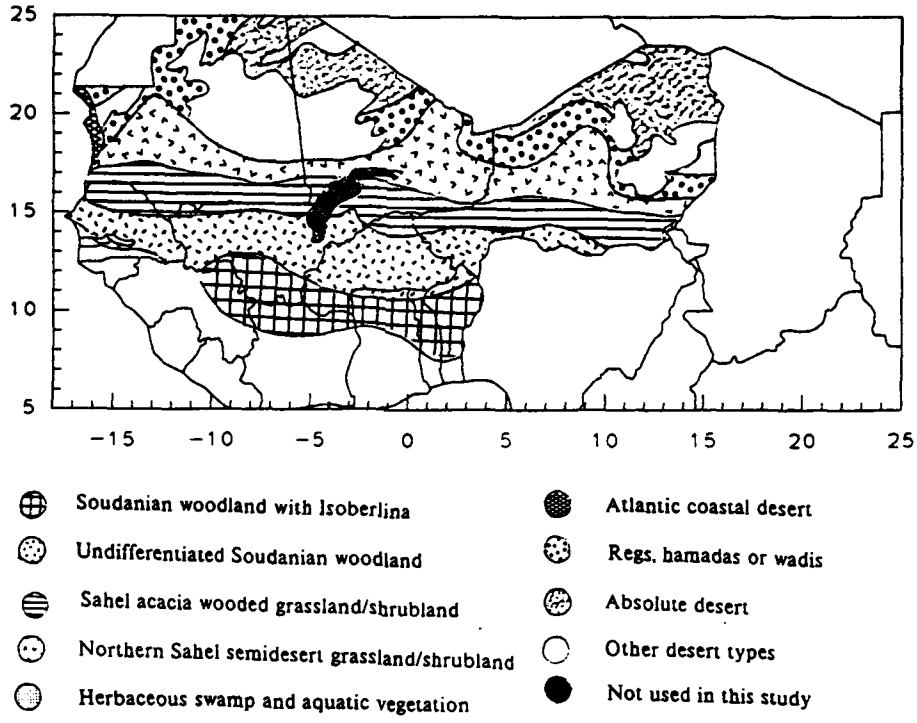

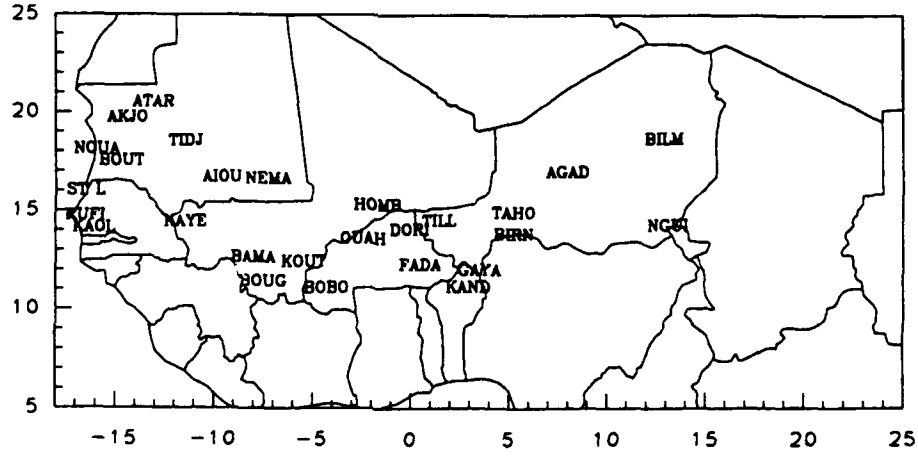

Figure 6: Map of vegetaion formations (after White, 1983) and station names.

Chapter 3

Spatial and Temporal Patterns

In this chapter, the spatial and temporal patterns of water vapor, aerosols (as inferred through aerosol optical thickness) and NDVI will be examined. An attempt will be made to see if changes in the patterns of water vapor and aerosols are consistent with the theory mentioned below.

It is hypothesized that the NDVI secondary peak is a result of fluctuations of atmospheric water vapor and aerosols. As mentioned in Chapter 1, increased water vapor decreases the NDVI signal and aerosols have a similar effect. In contrast, decreases in water vapor and aerosols cause an increase in the NDVI signal. It is known that as vegetation senesces during the dry season, the NDVI signal decreases. It is suspected that dry air, as is common in the region during winter and spring, can cause an increase in the NDVI. The harmattan, which brings the dry air into the region, also brings dust. The dust then decreases NDVI. This pattern of dry, then dry and dusty atmospheres, gives rise to a peak in the NDVI signal.

The time period of interest is that period from January to June. This time corresponds

to the dry season through to the beginning of the wet season. It was chosen because during this period NDVI should reach its minimum value, and peaks in the NDVI signal due to rainfall should be few.

3.1 Spatial and Temporal Patterns of the Secondary NDVI Peak.

Malo and Nicholson (1990) noted small secondary peaks in NDVI during the dry season for the stations they analyzed in Mali and Niger. By examining time series of stations, it appeared that nearly all of these secondary peaks occurred sometime between January and June. This was then chosen as the time period for examining the phase (timing) and magnitude of the peaks. The reasons behind this choice of time period were the seasonal cycle of water vapor and aerosols described before as well as the method of how to present the magnitude and phase. Generally, water vapor and aerosols reach their minimums during the first part of this time period, and then experience rapid increases toward the end of the period. The analysis is limited to months in which NDVI exceeds both the previous and following month's value. Four months with peaks are possible: February, March, April and May. This allows for a "vector" format presentation of the peak month, with the relative magnitude equal to the length of the vector and the direction corresponding to the month. The relative magnitude is defined as the amount NDVI in one month exceeds the average NDVI of the adjacent months. So for the four months mentioned, a vector pointing "east" indicates a secondary peak in February; vectors pointing north indicate a March peak; west

is an April peak and south is a May peak.

Figure 7 shows maps of this technique applied to forty-two stations in the region. A scale of .020 NDVI units is plotted in the upper right hand corner. Some stations have two vectors; this is because two separate peaks occurred during this time period.

The plot of 1982 in Figure 7 shows that February peaks (east pointing vectors) are of small magnitude and are located in Chad and Mauritania. Peaks in March are of moderate magnitude in northeast Niger and northern Mali with several more in Senegal and a few located in and around eastern Burkina Faso. April peaks appear to cluster in western Niger, eastern Mali and northern Burkina Faso. Another April cluster is located in Chad. These peaks are moderate in magnitude. May peaks are found in central Niger; a couple in Mauritania and a large magnitude in southern Burkina Faso.

The 1983 plot shows February peaks scattered, with small peaks in eastern Chad, a moderate peak in Nigeria; a moderate cluster in western Burkina Faso and other small peaks in Mali, Niger, Senegal and Mauritania. March has moderate magnitudes clustered from southwest Niger through Burkina Faso to northern Ivory Coast; some smaller magnitudes are found in Mauritania, northern Mali, northern Niger and two peaks are in Chad, one moderate. Magnitudes in April are moderate in Mauritania, central Niger and southern Chad with a strong peak in southwest Mali. May shows only two occurrences: one in Mali and a very weak one in Burkina Faso. 1983 is similar to 1982 in that peaks are spread out fairly evenly over the four month period.

The February peaks on the 1984 plot are of moderate to large magnitude and are clustered in Senegal and Mauritania; then decreasing in magnitude in western Mali. March has

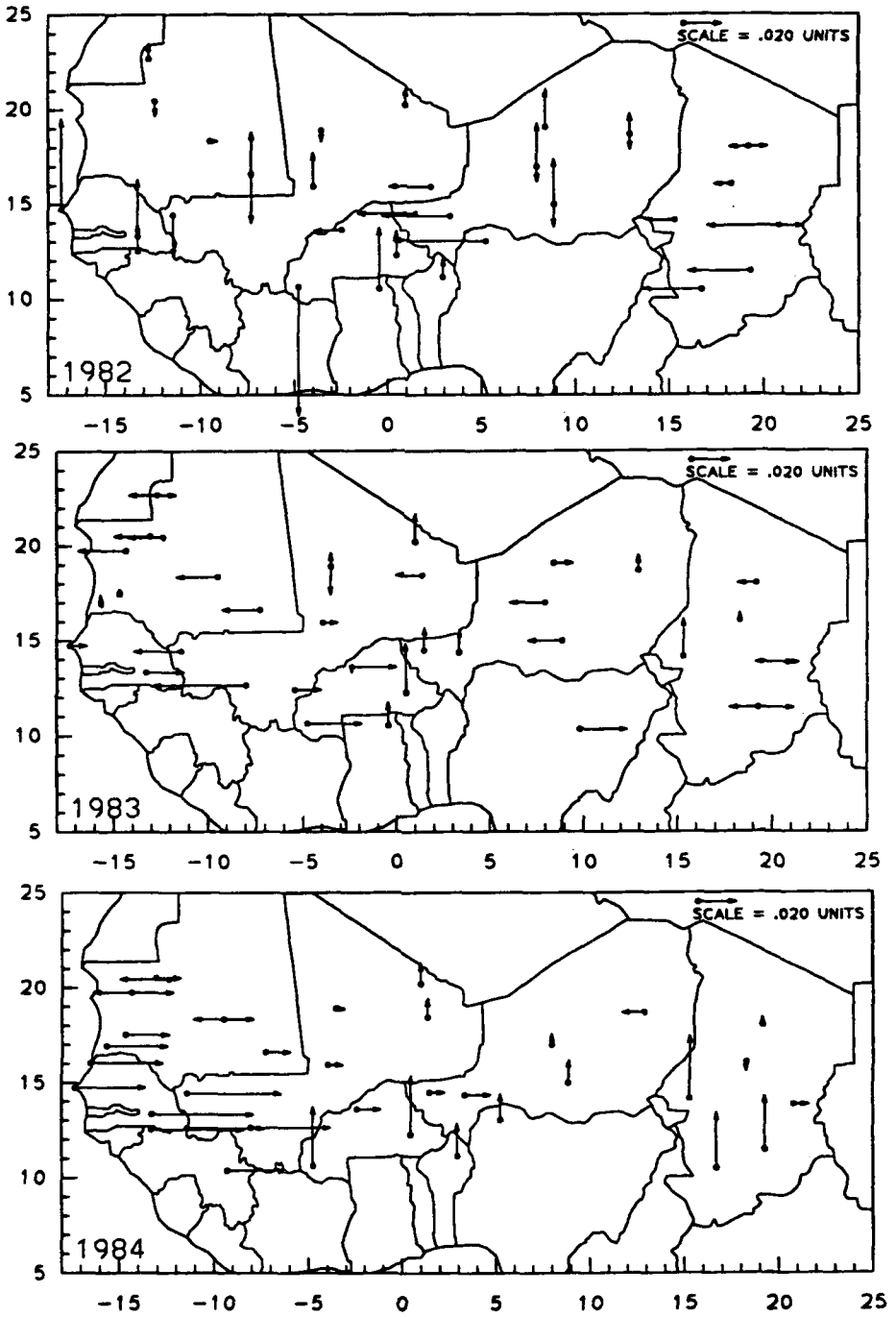

Figure 7: Plots of magnitude and phase of the secondary NDVI peak.→ represents peaks in February, ↑ represents March, ← represents April and ↓ represents May.

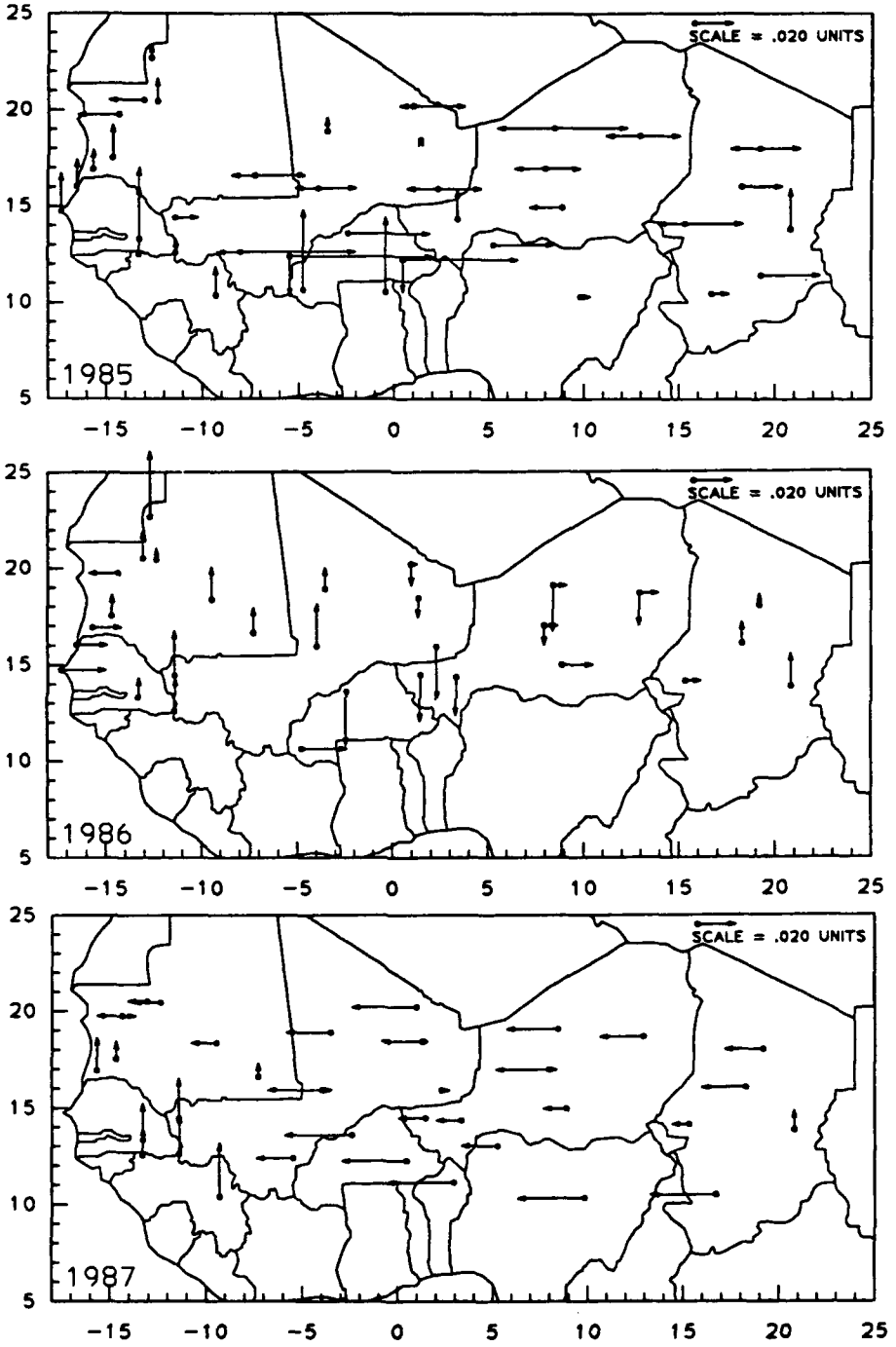

Figure 7: continued.→=February, ↑=March, ←=April, ↓=May.

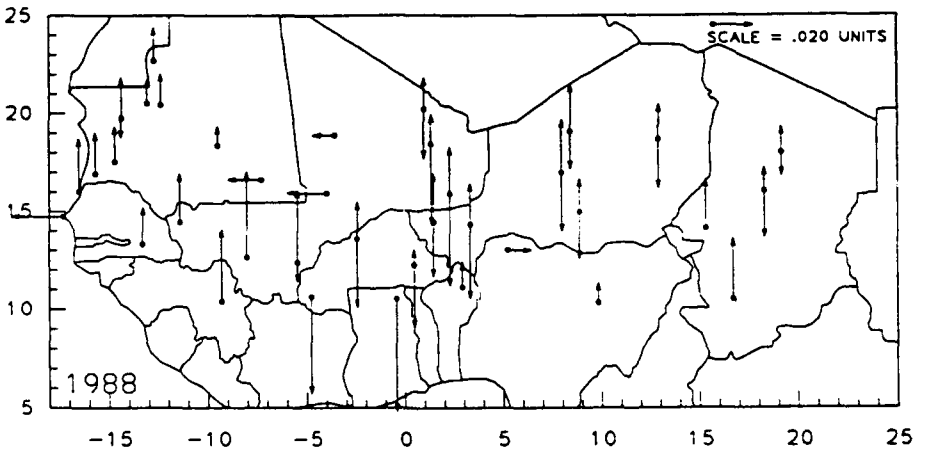

Figure 7: continued.→=February, ↑=March, ←=April, ↓=May.

moderate magnitudes along the southern border of the region from Burkina Faso east, with smaller peaks farther north in Mali. A few moderate April peaks are seen in Mauritania. May shows one minor peak in Chad. 1984 was different from 1982 and 1983 in having the majority of peaks in one month (Table 4).

In 1985, February shows very large magnitude peaks in southern Mali over to Burkina Faso. Other moderate February peaks are found in a band from eastern Mauritania over to Chad. March is represented by small magnitudes along the west coast, with larger magnitudes in southern Senegal, Burkina Faso and Ivory Coast. Other March peaks are in Guinea, Mali, Niger and Chad. April shows a broad band of weak to moderate magnitude peaks from the northern half of Chad through to west central Chad. Only two May peaks are found; one each in Mali and Burkina Faso.

1986 had the distinction of the fewest secondary peaks in this analysis. February had

fairly weak magnitudes along the west coast; weaker still in northern Niger and a moderate loner in Burkina Faso. March had moderate peaks in a band from northern Mauritania over to Mali and down to Guinea with other peaks in Chad. Only one April peak is seen: in western Mauritania. May had moderate magnitudes extending, while decreasing in magnitude, from Burkina Faso up into Niger.

1987 was a fairly uniform year. There were only four peaks in February, all very small, located in Mauritania, Mali and Niger. March has a cluster of moderate peaks extending southeast from Mauritania to Guinea with a lone peak off in Chad. April was the dominant month in 1987, with moderate magnitude peaks extending in a broad, nearly unbroken band from Chad to west central Mauritania. May had no peaks.

1988 was another year when one month dominated, but it was a different month than in 1987. Only one peak occurred in February, and it was in Nigeria. March peaks, however, occurred in a broad band from western Mauritania to Chad, with some larger magnitudes in southern Mali. This is similar to the pattern seen in 1987 for April. April 1988 had four peaks, moderate in magnitude, with three clustered near the Mauritania/Mali border and one at Dakar. May was the other "active" month in 1988, with a band extending northeast from Burkina Faso up through Mali and Niger. May peaks in southern Burkina Faso and Ivory Coast had large magnitudes.

Table 4 shows a breakdown of the occurrences of the peaks by month and year. The table shows interesting patterns. In 1982, 1983, 1985 and 1986, three of the months had much higher percentages than the fourth, which had less than 10% of the peaks. This pattern occurs in most years, with the exception of 1984, 1987 and 1988. In these years,

one month out of each year had more than 50% of the peaks, and April 1987 had 65% of that year's peaks.

Table 4: Occurrence of Peaks by Month and Year

Year	Month, Percent of Total				Month, Total # of Peaks				Total
	Feb	Mar	Apr	May	Feb	Mar	Apr	May	
1982	8	39	31	22	3	14	11	8	36
1983	29	29	37	5	11	11	14	2	38
1984	54	32	11	3	20	12	4	1	37
1985	40	30	26	4	20	15	13	2	50
1986	29	41	3	26	10	14	1	9	34
1987	11	24	65	8	4	9	24	0	37
1988	2	58	8	33	1	30	4	17	52
Avg	24	40	25	14	9.8	15	10.1	2	41.2
Total					69	105	71	14	289

3.2 Spatial and Temporal Patterns of Water Vapor

In this section, the spatial and temporal patterns of water vapor will be presented using contoured maps. The maps will show contours of values of precipitable water as derived from equation (3) and applied to the water vapor data of the 27 stations previously mentioned.

Ben Mohamed and Frangi's 1986 study showed that, for the Sahelian region, precipitable water is very closely related to surface water vapor pressure. This is because in this region most of the moisture is near the surface, while much drier air is found aloft (Dubief 1979). Precipitable water is shown because it provides a measure of total atmospheric water content. Knowledge of this parameter is required since the NDVI is computed from signals which pass through the entire atmosphere.

Figures 8a-l are the contour maps of precipitable water. The discussion will focus on

the maps for January through June as this is the period of interest. Figure 7a shows the average January pattern of precipitable water (Pw), for the seven year period 1982-88. It is a simple pattern with nearly all areas having Pw values less than 1.5cm for the month. The gradient is tightest along the west coast, where values of approximately 2.5cm are found. Values below 1.0cm are found at the northern edge of the region.

The February (Figure 8b) pattern is slightly different from the January pattern. The gradient near the west coast remains in place. A tongue of Pw values greater than 1.5cm extends into southwest Niger. The area of values less than 1cm found in the north in January has retreated in February.

The March (Figure 8c) pattern is similar to the February pattern. The gradient along the west coast remains, while values of Pw at the coast have increased to 3cm. The bulge of moisture in southwest Niger is also present. Values of Pw at the southern edge have increased to 2.5cm. The minimum along the Senegal-Guinea border appears to be a result of the contouring subroutine.

In April (Figure 8d), the patterns of Pw begin to change. The gradient in the south has become much tighter, with values at the extreme south reaching 4.0cm. The 3.0cm contour appears in Guinea through to Nigeria. This contour is closely associated with the position of the ITCZ. The west coast gradient remains relatively unchanged. The 1.5cm contour has moved north approximately 2 degrees of latitude. Interestingly, the dry values (Pw less than 1.0cm) have returned in the north.

In May (Figure 8e), the 3.0cm contour has moved north about 2 degrees. The moisture in the south has continued to increase with values of Pw now near 5.0cm. The west

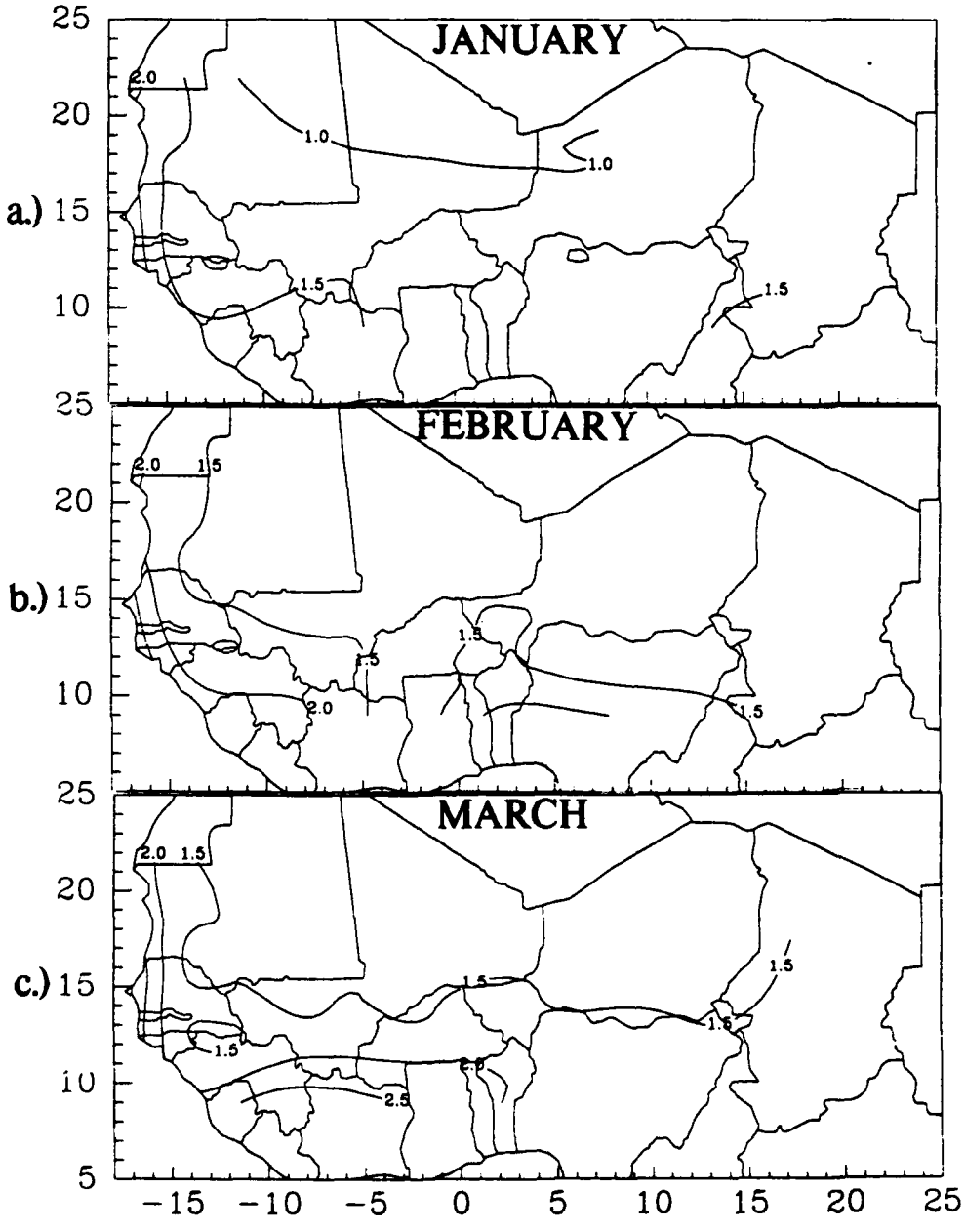

Figure 8: Contour maps of precipitable water

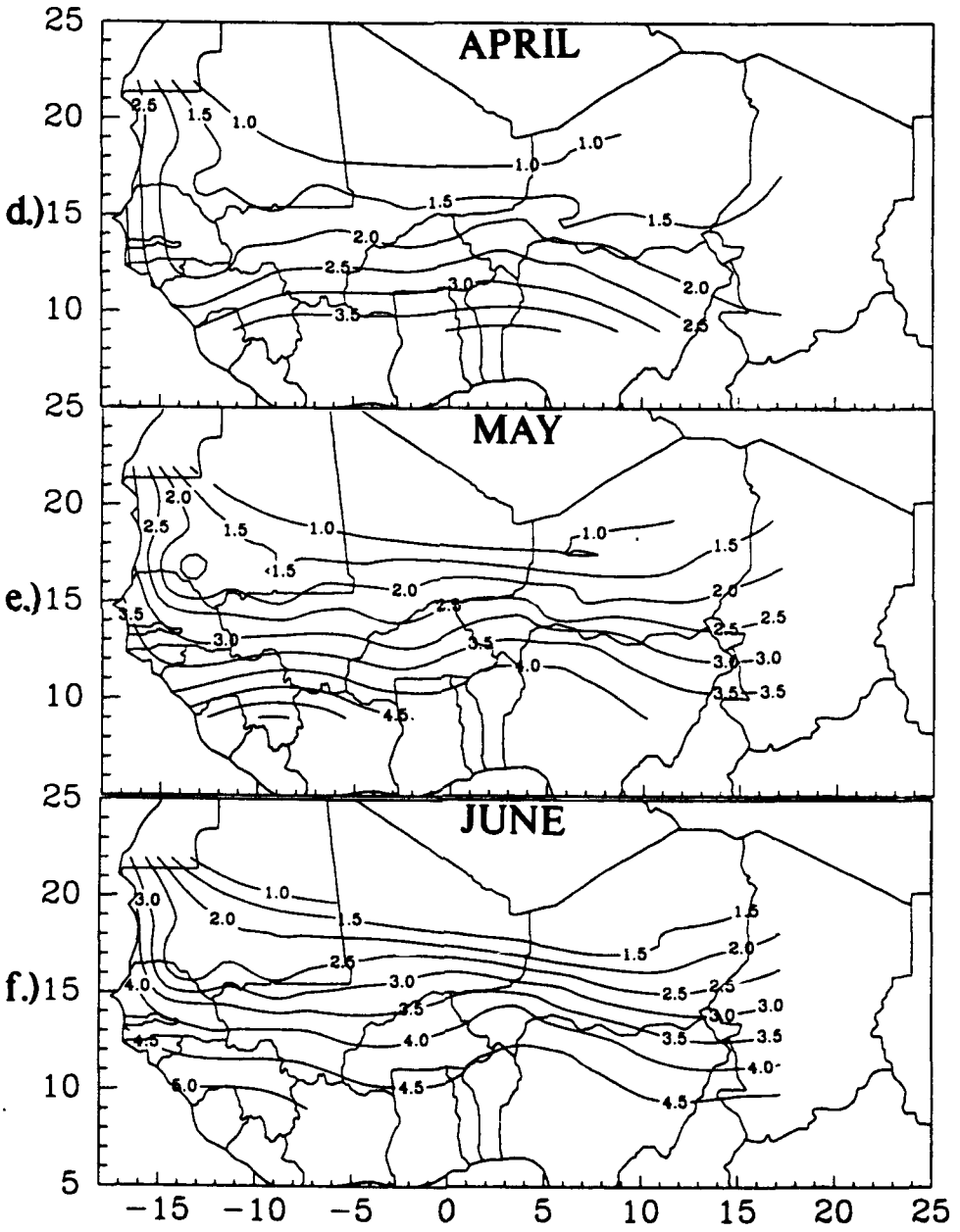

Figure 8: continued.

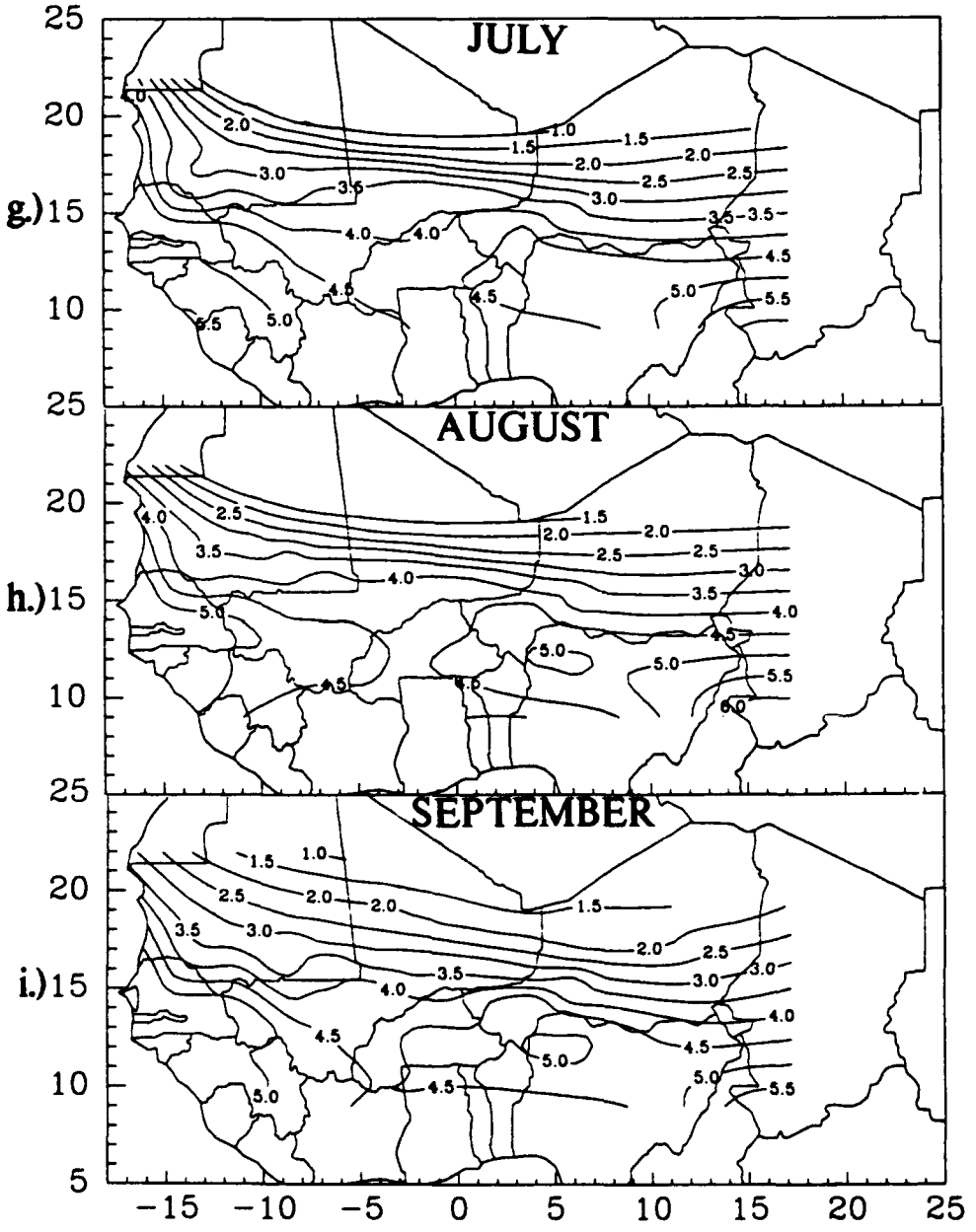

Figure 8: continued.

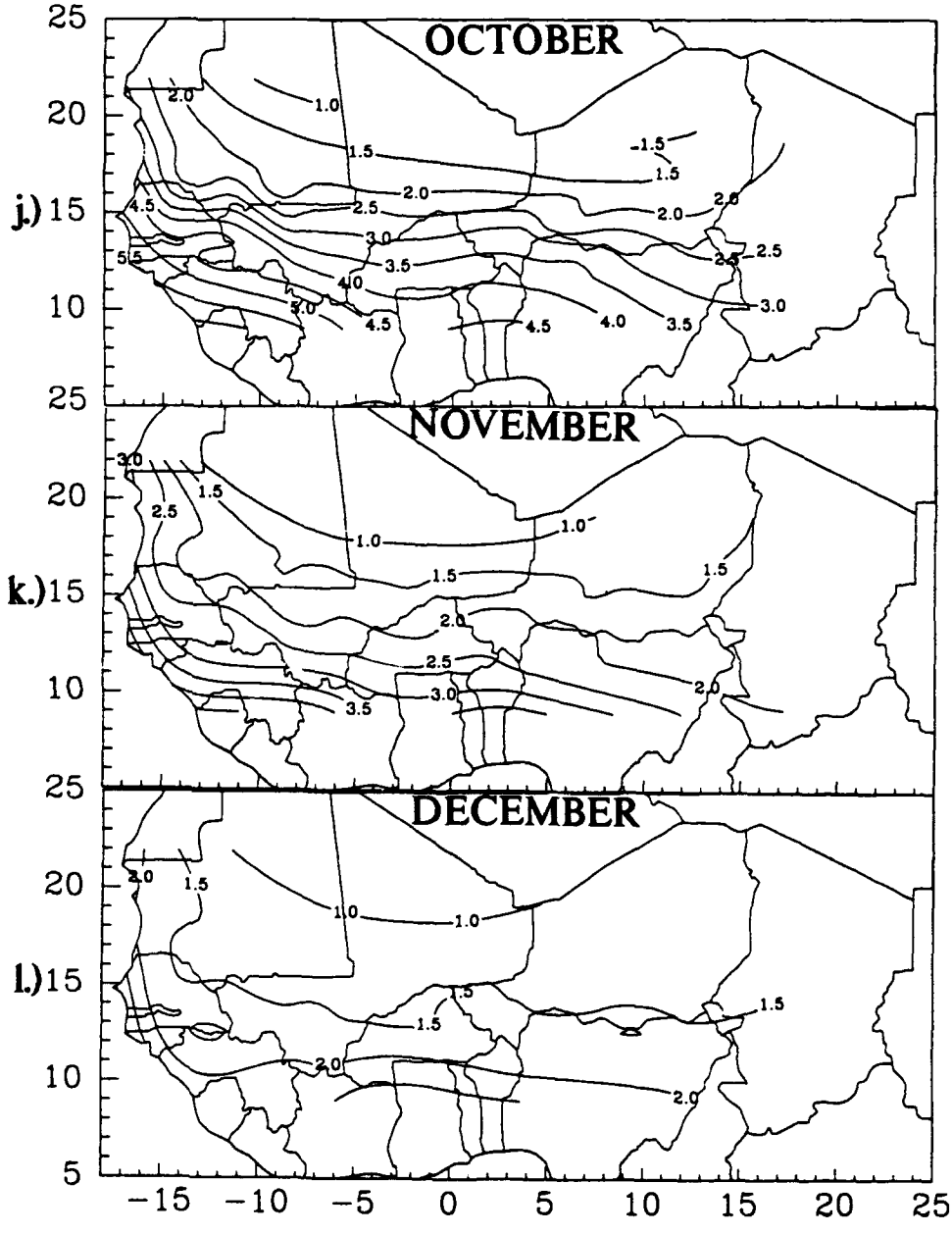

Figure 8: continued.

coast gradient has steepened, with values above 3.5cm at the coast and dropping to less than 2.0cm inland. The minimum in southwest Mauritania appears to be a result of the contouring routine. While data suggest lower values in the area, the closed contour is a result of interpolating values between stations. The area in the north with Pw less than 1.0cm remains.

The June (Figure 8f) pattern shows that moisture has moved well into the region. The 3.0cm contour has moved north approximately 2 degrees. Moisture on the west coast has increased to about 4.5cm, while in the south 5.0cm is the maximum.

Since this study is mainly concerned with the latter portion of the dry season, the period of July through December will be discussed only briefly. In the remaining figures (8g-l), the advance of the ITCZ can be traced by following the 3.0cm contour. That contour can be seen advancing northward in July. In August, as the ITCZ has reached it northernmost position, the 3.0cm contour has ceased its progression north. In September, the 3.0cm contour and the ITCZ begin to retreat southward, so that by December, the 3.0cm contour and the ITCZ are both out of the region.

Examining the plots of magnitude and phase of the secondary peaks along with monthly plots of contoured water vapor pressure (not shown) revealed, at best, inconclusive results. In 1986, for example, March water vapor plots showed unusually dry air around clusters of March peaks in Mauritania. Water vapor plots are nearly identical to precipitable water, which was derived from water vapor pressure by (3). However, May water vapor plots showed higher than average water vapor (for the seven year period analyzed) near the May peaks in Burkina Faso, Mali and southern Niger.

The above example exemplifies the problems of the different types of data sets. Without daily water vapor data, most of May could have been unusually moist, but one clear, dry day, when the satellite passed nearly overhead, could have produced that month's maximum NDVI value. Obviously one must be very careful when attempting to explain the causes of the secondary peak.

3.3 Spatial and Temporal Patterns of Aerosols

Describing the spatial and temporal patterns of aerosols is one of the more difficult tasks of this study. The reason for this difficulty lies in the limited number of studies which have been made on the subject. Holben *et al.* (1991) listed published sun photometric studies conducted in the Sahel. These are shown in Table 3 along with some more recent studies. The longest continuous measurements were made by D'Almeida (1987) and lasted for 24 months. Yet this was only for two stations in the region, Agadez and Gao. Ben Mohamed *et al.* (unpublished manuscript) did a sun photometric study for seven stations in Niger which covered eighteen months. In all, measurements have been made at only thirteen stations in this region and only sporadically in time.

3.3.1 Sun Photometry

In all the studies previously mentioned, the aerosol optical thickness was measured using sunphotometers. A sunphotometer uses interference filters and a photovoltaic silicon detector to determine solar radiation transmitted through the atmosphere. The interference filters detect selected wavelength bands, while the silicon detector registers current on a

Table 5: Summary of Sun Photometer studies conducted in the Sahel. (After Holben *et al.* 1991)

Authors	Coverage	Temporal	Notes
D'Almeida (1986,1987)	Spatial	2 years+	11 stations very widely separated
Ben Mohamed and Frangi (1983, 1986)	Point	14 months	Limited to Niamey
Ben Mohamed *et al.* (unpublished manuscript)	Spatial	18 months	7 stations in Niger
Oluwafemi (1979)	Point	1 dry season	Limited to Lagos
Cerf (1980)	Spatial	3 years	5 widely separated stations, sporadic observations
Fouquart *et al.* (1987)	Point	2 months	Limited to near Niamey

micro-ammeter. Then, using the Lambert-Beer Law

$$V = (V_o/r^2)\exp(-\tau_t m) \tag{4}$$

where V is the voltage measured, V_o is the spectral voltage at the mean Earth-Sun distance, r is the mean Earth-Sun distance, τ_t is the total optical thickness and m is optical airmass. The aerosol optical thickness, τ_a, is then equal to:

$$\tau_a = \tau_t - (P/P_o)\tau_r - \tau_o \tag{5}$$

where P is the station pressure, P_o is standard sea level pressure, τ_r is the Rayleigh optical thickness at standard pressure and τ_o is the ozone optical thickness (Holben *et al.* 1991). Values for τ_r and τ_o are taken from various sources such as Pendorf (1957), Junge (1963) or Braslau and Dave (1973).

In order to determine the turbidity parameter, β, also used to describe a dusty atmosphere, Angstrom's wavelength exponent, α, must be found. The relationship is

$$\alpha = \ln(\tau_{a1}/\tau_{a2})/\ln(\lambda_1/\lambda_2) \tag{6}$$

where λ_1 and λ_2 are wavelengths (Holben *et al.* 1991), and τ_{a1} and τ_{a2} are aerosol optical thickness. The turbidity parameter, β, is then determined by

$$\tau_a = \beta\lambda^{-\alpha}. \tag{7}$$

Different studies use different wavelengths. Ben Mohamed and Frangi (1986) used 350, 380, 440, 500, 641, 876, 1024, and 1610nm wavelengths. Oluwafemi (1979) used 500, 880, and 940nm. Cerf (1980) used 506 and 880nm. Holben *et al.* (1991) used 500, 640, 875 and 940nm. Each of these values corresponds to the center of a wavelength band, whose half-width is typically 5nm. Values of aerosol optical thickness (τ_a) vary with respect to wavelength. Ben Mohamed and Frangi (1986) found differences in τ_a of up to .4 for wavelengths of 350 and 1610nm. However, Holben *et al.* (1991) found τ_a to be nearly identical for different wavelengths at any given time. The reason for this discrepancy is unclear.

3.3.2 Description of Aerosol Patterns

The Sahara is the source region for most aerosols affecting the study area. Kalu (1979) has suggested two main areas for the production of dust are the alluvial plains of Bilma-Faya Largeau and the area west of the Ahaggar Massif (Figure 9). Factors such as surface soil texture, wind speed, vegetation, vegetative residue, surface roughness, soil aggregate size

distribution and soil moisture all determine dust production. Kalu (1979) and Dubief (1979) both describe three main weather patterns which can produce dust or dust storms. In the winter, these are upper level troughs (@ 200mb) followed by surface ridging or polar fronts and associated post-frontal pressure rises. The pressure rises in turn tighten the gradient and can cause winds of 30 to 50kts. In the summer, the weather systems are easterly waves with associated thunderstorm activity. The downdrafts from these storms lift large quantities of dust into the atmosphere.

Figure 10 shows a map of stations for which aerosol data was available. This data came from four of the studies listed in table 3. These four are: Ben Mohamed *et al.* (unpublished manuscript), Holben *et al.* (1991), Cerf (1979) and D'Almeida (1987). Time series of the data are shown in Figure 11a-d. Upon examining Figure 11, it becomes obvious that the spatial and temporal patterns are very complicated. Not enough stations had contemporaneous data to facilitate contouring. Still, a pattern of generally high aerosol optical thickness (or turbidity) from spring through summer and lower aerosol optical thickness in fall and early winter can be seen. The plots also show, however, that during these seasons aerosol optical thickness can vary substantially. Location next to an assumed source region does not always guarantee the most aerosols. In the Ben Mohamed *et al.* data (Figure 11a), Bilma, supposedly in one of the source regions, has lower τ_a than Zinder does for the 1986 period, and Zinder is more than 750km from the source.

In another case, Birni N'Konni and Tahoua, (Figure 10) which are separated by only 100km, have very different τ_a values (Figure 11). In fact, Tahoua, the station closer to the Sahara, shows decreasing τ_a from September to November while Birni N'Konni to the

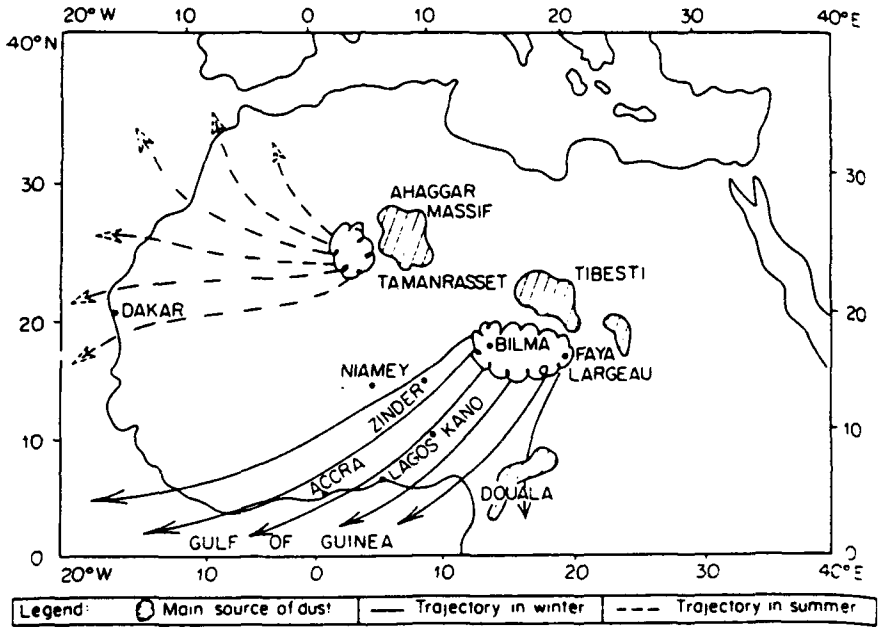

Figure 9: Dust soure regions in West Africa (from Kalu, 1979).

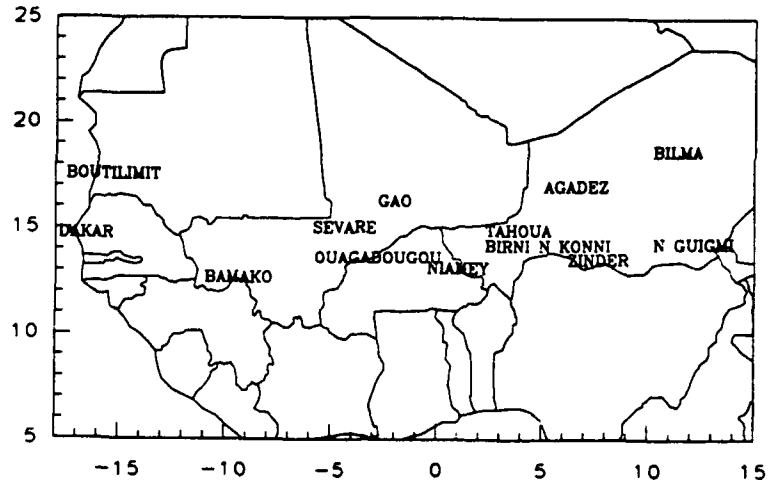

Figure 10: Stations at which sun photometric studies have been done.

sensing of vegetation. In the case of Birni N'Konni and Tahoua mentioned above, τ_a was 65% greater only 100km to the south. Clearly, this increase in aerosol content will affect the value of NDVI. Chapter 5 will describe the attempt to correct for these differences in aerosol loadings.

In order to say with more certainty that a peak was caused by changes in water vapor and aerosol content, it would be necessary to know the date that the monthly NDVI value was obtained. Then, examining water vapor and aerosol tendencies around the time of retrieval of the NDVI signal could indicate if water vapor and aerosols caused an enhanced NDVI signal. Unfortunately, those data are not readily available, especially in the case of aerosols, for which data is extremely limited.

A somewhat unrelated, but worthy of note, point needs to be made about the time

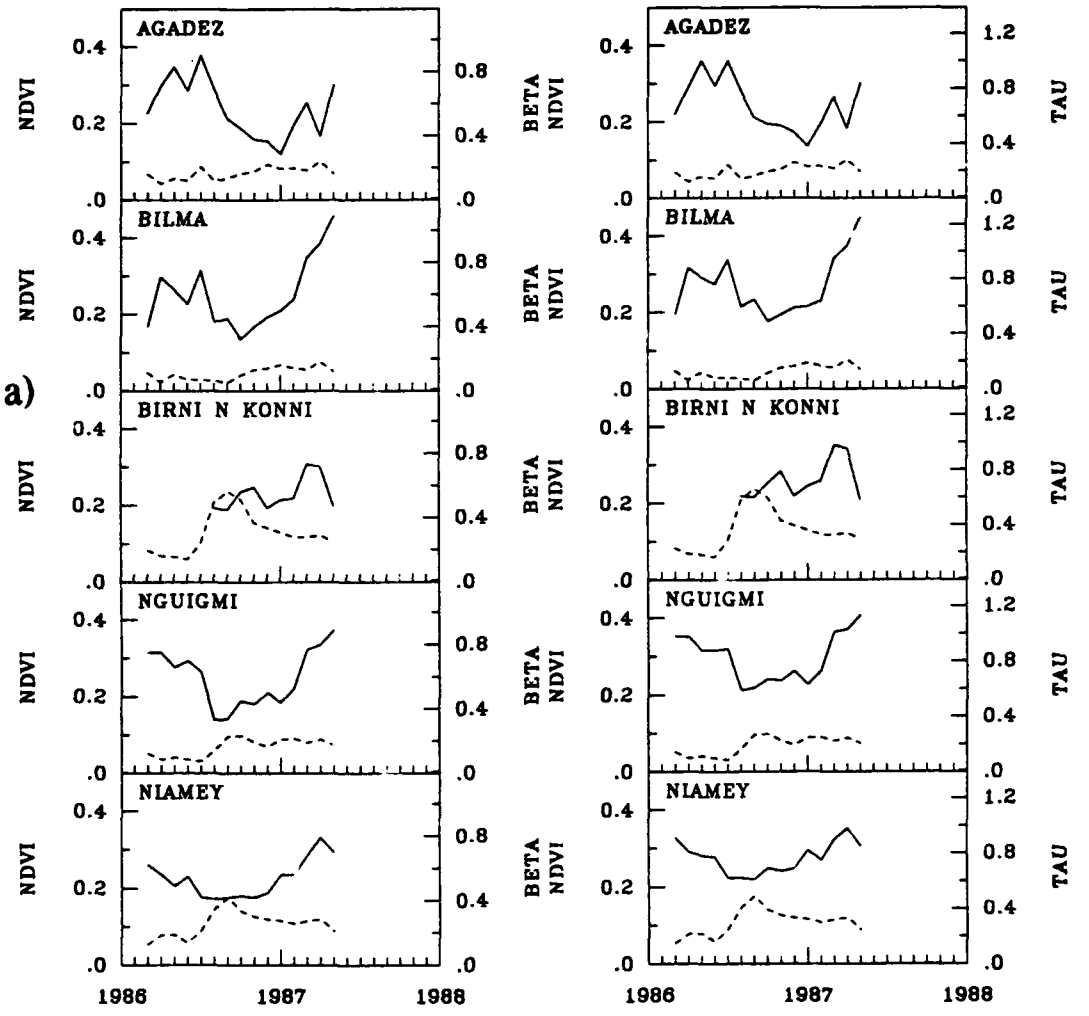

Figure 11: Time series of aerosol optical thickness, τ_a, or turbidity, β (a) after Ben Mohamed *et al.* solid line is τ_a, dashed line is NDVI, unpublished manuscript; b) Cerf, 1979; c) D'Almedia, 1987; and d) Holben *et al.* 1991).

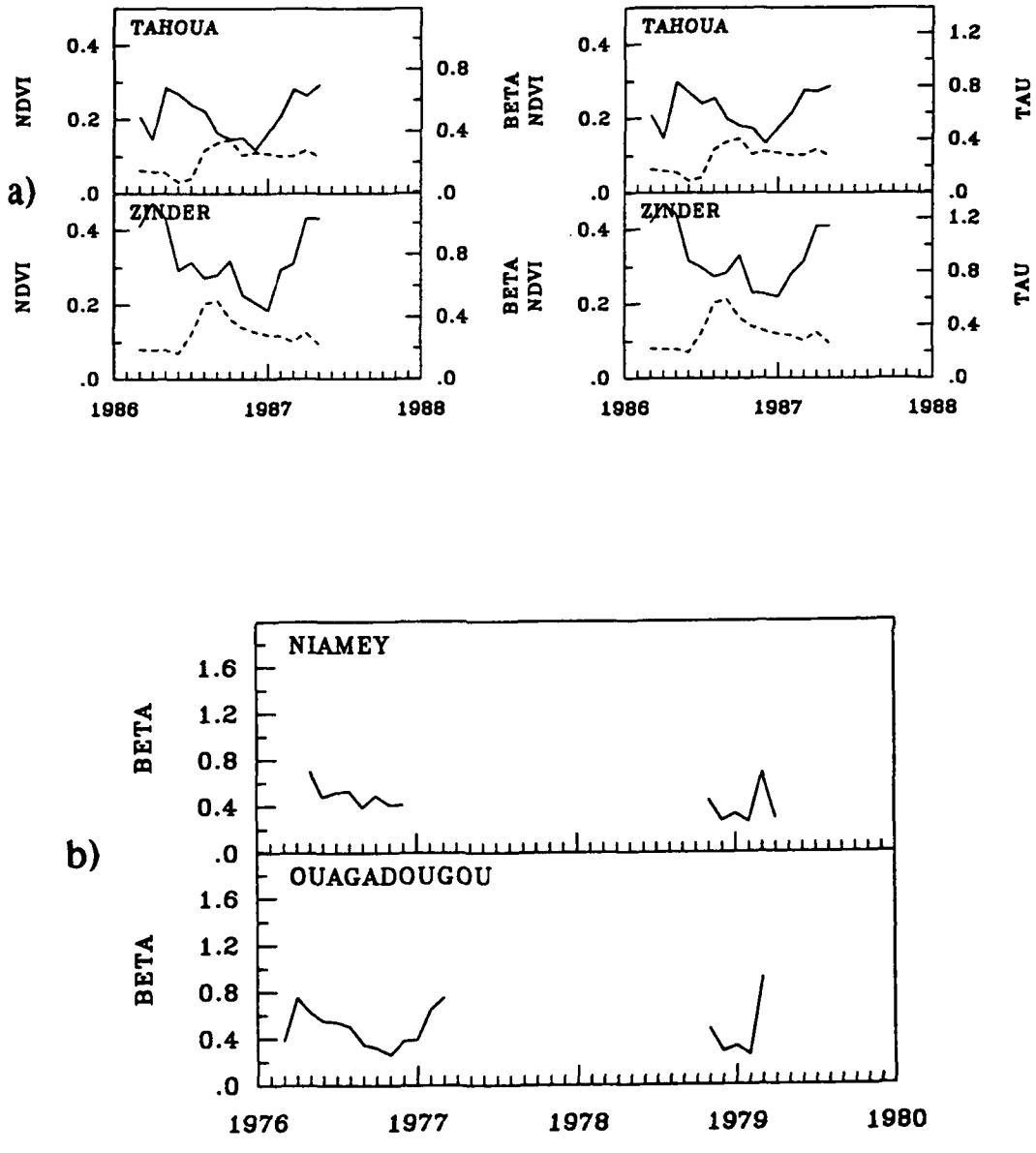

Figure 11: continued.

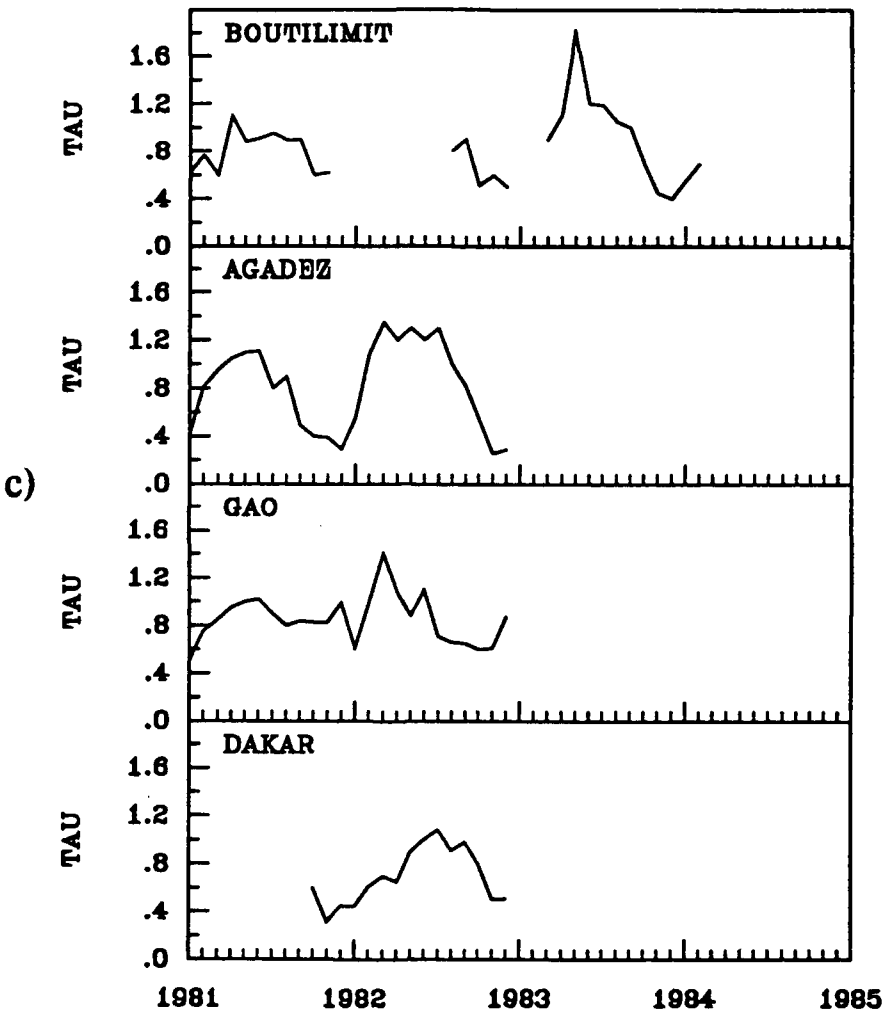

Figure 11: continued.

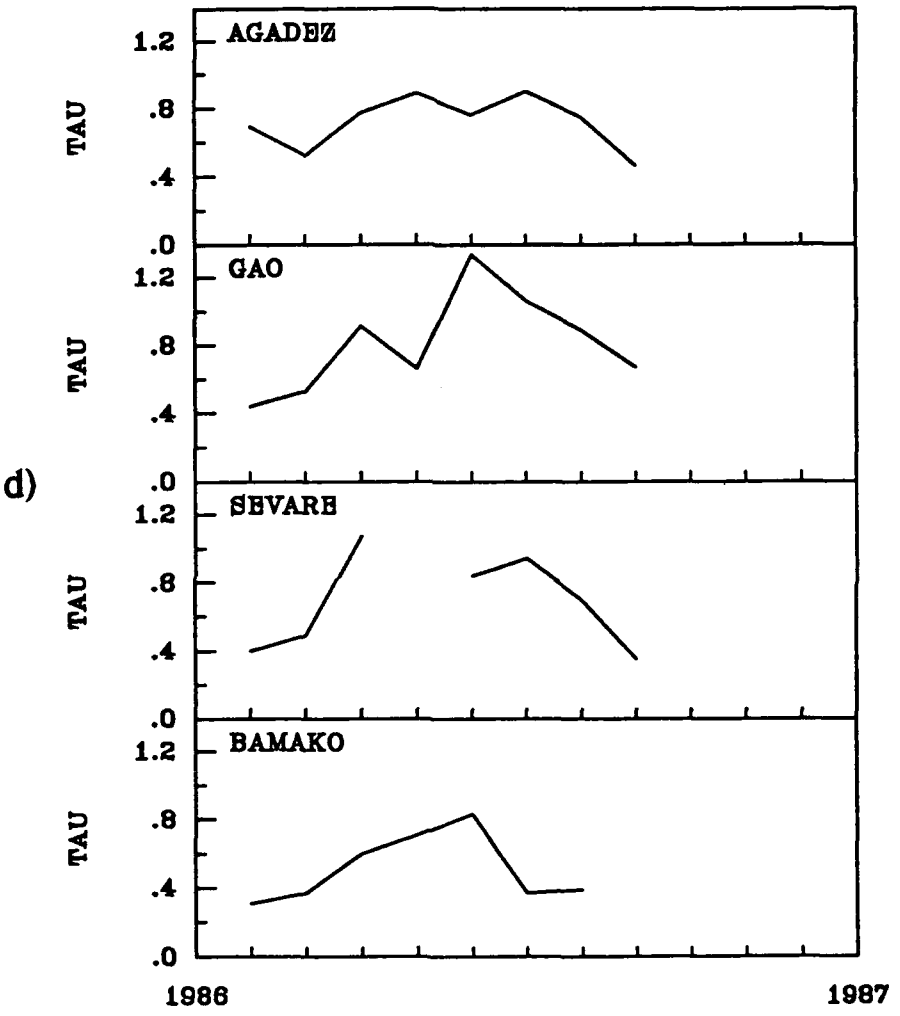

Figure 11: continued.

A somewhat unrelated, but worthy of note, point needs to be made about the time series shown in Figure 5. By examining the time series, it can be seen that the NDVI curves exhibit an upward trend. Lare (1992) also noted the upward trend of NDVI when comparing time series of NDVI with time series of soil moisture and evapotranspiration for stations in West Africa. It is unclear what causes this trend but it may be related to inter-satellite calibration or processing of the global area coverage data.

Chapter 4

Correlation Studies

In order to further study the relationship between NDVI and water vapor, a correlation study was done. Using Pearson's correlation, NDVI anomalies were correlated with surface water vapor pressure anomalies for each of the 27 stations for which water vapor data was available. Anomalies were calculated by determining monthly means for the seven year period 1982-1988 and subtracting the appropriate mean from each month in the period. NDVI and water vapor anomalies are plotted in Fiqures 12 and 13. The five stations represent a cross-section from northwest to southwest across Niger into Burkina Faso and can be seen in Figure 14. Upon examining Figure 12, it is obvious that NDVI anomalies are larger in the more southern stations (i.e. Tahoua, Dori and Bobo Dioulasso). These stations have higher annual rainfall and more vegetaion growth. They are also in a region in which Tucker *et al* (1991) showed to have a large coefficient of variation.

All stations display an upward trend as noted previously. Several stations experienced higher rainfall at the end of the seven year period than at the beginning and this may

explain the trend. The trend may also be related to inter-satellite calibration or processing of the global area coverage data.

Correlations were done for the seasons during which the secondary NDVI peak occurred. In West Africa, there are four seasons: the dry season (December-March); the transition to wet season (April-May); the wet season (June-September) and the transition to dry season (October-November). Correlations are shown in Figure 14 for the dry season and the transition to wet season. This corresponds roughly to the period of time in which the magnitude and phase of the secondary peak was described. Stations with correlations which did not exceed the 95% confidence level are represented with a dot.

For the dry season (December to March), virtually all stations show water vapor anomalies to be uncorrelated with NDVI anomalies. If water vapor were primarily responsible for altering the NDVI signal as some have suggested (Huete and Tucker 1991, Tucker *et al* 1991) one would expect a stronger negative correlation. Since water vapor content is lowest at this time of year (Figure 8), the effect of water vapor on NDVI should be lowest at this time also. It may be that the other influences on the NDVI, e.g. illumination geometry, soil influences and aerosols, have a similar magnitude effect as water vapor during this season.

In the transition to wet season, a larger number of stations have signifigant correlations. All correlations are negative, with a r=-.825 at Birni N'Konni. It appears at this time, as water vapor is increasing with the advance of the ITCZ, NDVI begins to decrease. Since water vapor increases preceed rainfall, vegetation has not yet begun to grow. Thus, the influence of water vapor is stronger than the other factors affecting NDVI.

Correlations for the remaining seasonal and annual time periods (not shown) generally

showed poor correlations. The reason for this is unclear, since one might expect the effect of water vapor to be seen throughout the year. However, since so many factors affect NDVI, it is probable that the water vapor signal is only dominant in the transition to wet season. The reason water vapor correlates poorly in the wet season is that as vegetation grows, it responds to different rainfall amounts which are not necessarily related to increased or decreased water vapor content (Lamb 1982). In this way, fluctuations in vegetation due to precipitation exceed fluctuations which might be caused by atmospheric water vapor.

Another method of removing the seasonal effects was to do a seven month running average of the anomalies. These running means are shown in Figure 15, and tend to show an out of phase relationship. This smoothed data set was then correlated for the entire period. These correlations are shown in Figure 16, with correlations below the 95% confidence level represented by a dot. The correlations in Mauritania are quite high in some instances, with r=-.918 at Atar. These results show the out of phase relationship between NDVI and water vapor which points to water vapor's effect on NDVI, that is, increased water vapor decreases the NDVI. However, some correlations were positive, particularly in southern Mali, along the Atlantic coast (at Rufisque) and in northern Niger (at Bilma). It is unclear why the positive correlations occur, however it may be due to other influences such as proximity to the ocean (Rufisque) or soil influences (Bilma).

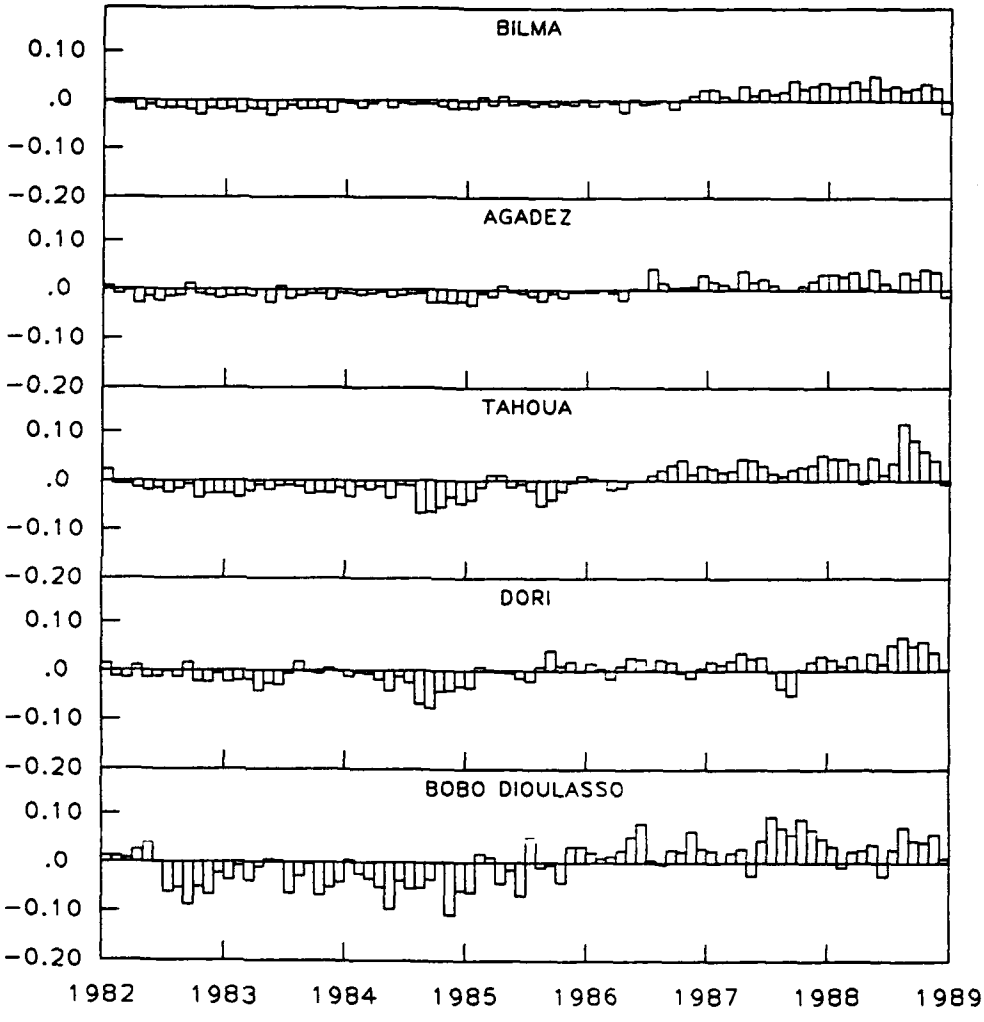

Figure 12: Plots of monthly NDVI anomalies.

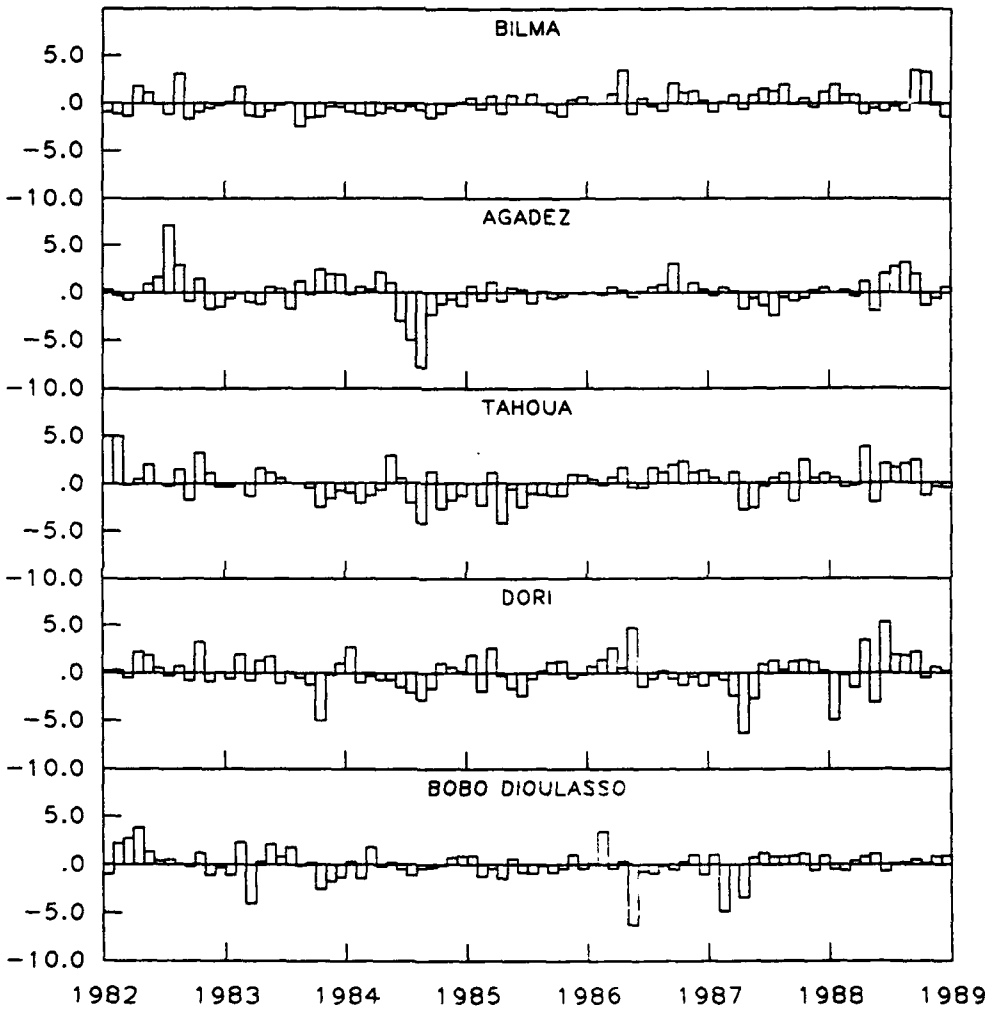

Figure 13: Plots of monthly water vapor anomalies.

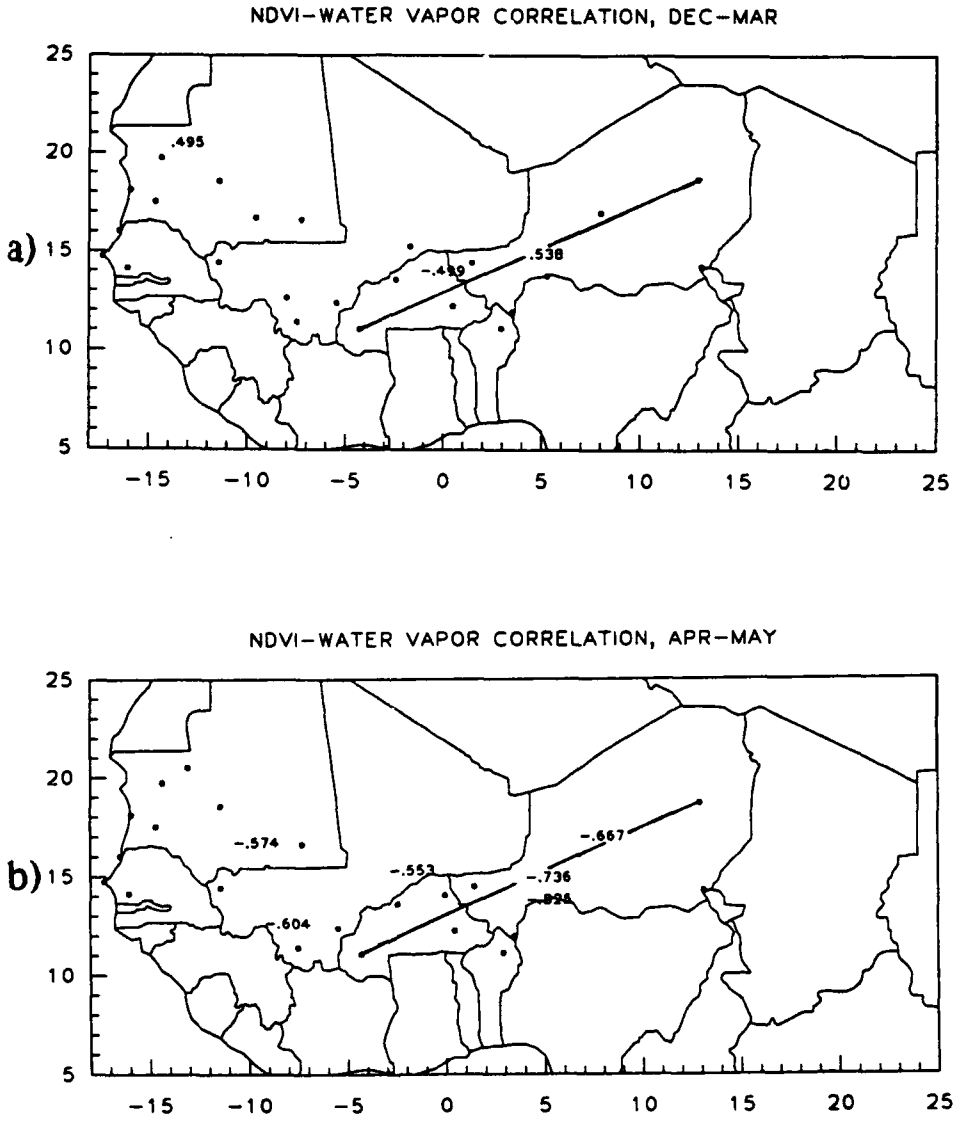

Figure 14: Plots of NDVI-water vapor anomaly correlations for a) dry season (December-March) b) transition to wet season (April-May). Line represents cross-section of stations shown in previous figures.

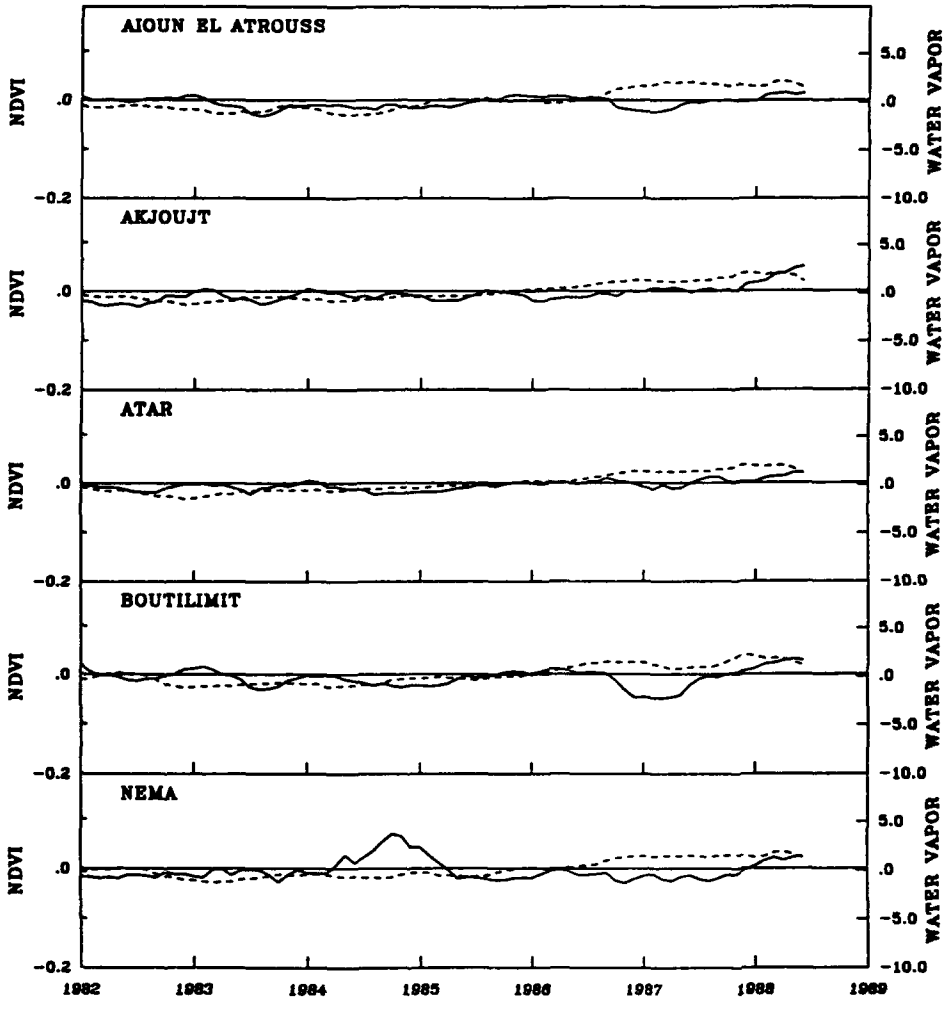

Figure 15: Plots of seven month running means of NDVI anomalies (dashed line) and water vapor anomalies (solid line) for selected stations in Mauritania.

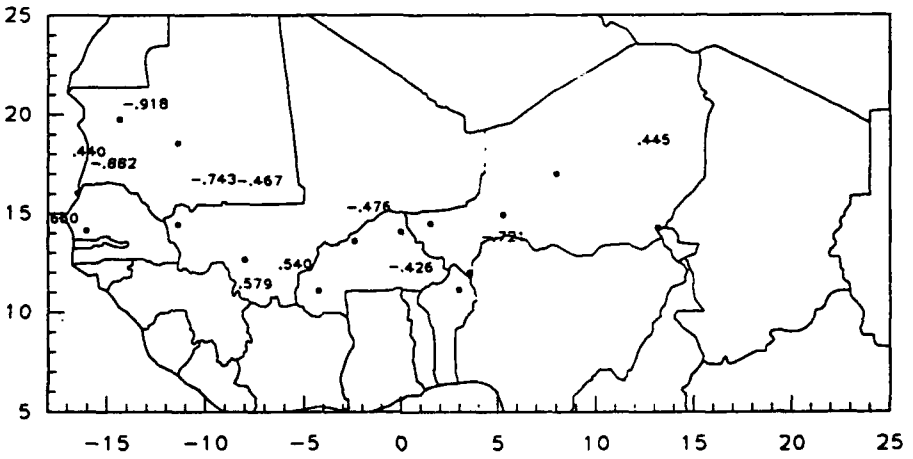

Figure 16: NDVI-water vapor anomaly running mean correlations.

Chapter 5

Corrections for NDVI

Recently, several authors have published their results of changes in NDVI due to either water vapor or aerosols as calculated by radiative transfer code. In particular, articles by Justice *et al.* (1991) and Holben *et al.* (1991) are especially relevant to the subject of atmospheric corrections for NDVI in the Sahelian region. These studies are the foundations of the corrections which are applied to NDVI in this study.

5.1 Corrections of NDVI for Water Vapor

The Justice *et al.* (1991) study examined the effects of water vapor on the NDVI signal. They modeled surface reflectance as seen by the AVHRR in the satellite. In their model water vapor was assumed to be beneath aerosols which is consistent with Sahelian conditions (Dubief 1979).

The Justice *et al.* (1991) study modeled the change in NDVI ($\Delta NDVI$) for varying

amounts of water vapor. A line was fitted to their data points (Figure 17), and a log-linear regression equation was developed. The equation is

$$\Delta NDVI = -.04 - .02 \log(Pw) \tag{8}$$

where $\Delta NDVI$ is the change in NDVI due to Pw, atmospheric water vapor content in centimeters. The regression equation was applied to the 27 station NDVI data set for which water vapor data was available. Figure 18 shows plots of all 27 stations' NDVI, "corrected" NDVI, precipitable water and $\Delta NDVI$.

One purpose in correcting the NDVI for water vapor effects was to see if, once corrected, the secondary peaks described in Chapter 3 could be reduced or eliminated. The corrected NDVI was subjected to the same analysis described in section 3.3. A comparison was then made of the months (i.e. February, March, April and May) with peaks occurring in NDVI versus corrected NDVI. Figures 19a-e are plots of the average percent reduction of the peak for each month of the seven years. The February plot (Figure 19a) shows mixed results. While peaks were reduced more than 50% in Bilma, Agadez and N'Guigmi, peaks were increased (negative values on the figure) by 50% in magnitude at Atar. Other increased magnitudes were found elsewhere in Mauritania, as well as Senegal, Mali and Burkina Faso, for a total of ten stations.

The March plot (Figure 19b) shows slightly better results. Only four stations experienced increased magnitudes, with a 47% increase at Tahoua. Otherwise, a reduction of the peak by 20% of more was common.

The April plot (Figure 19c) still shows a couple of increased magnitudes, such as a 16%

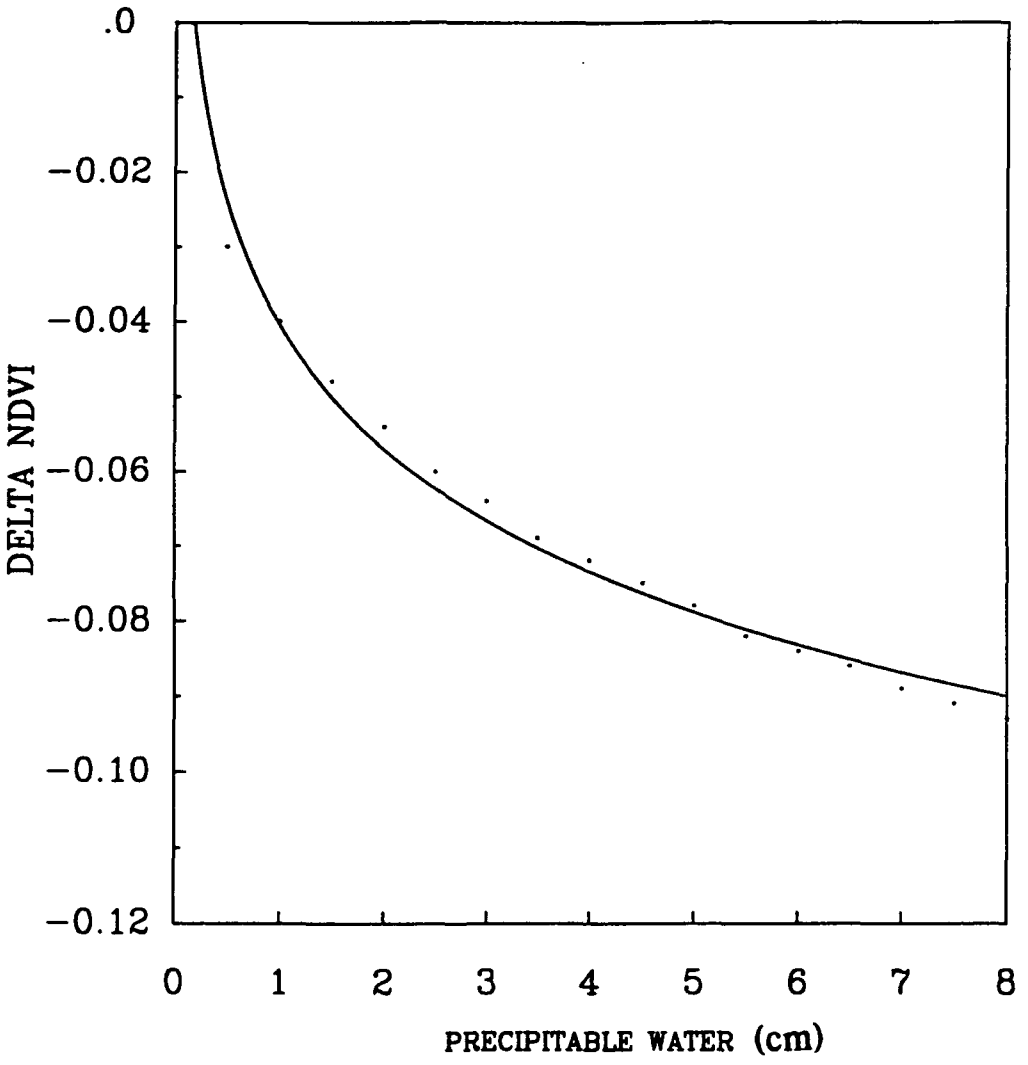

Figure 17: Plot of regression of Delta NDVI with precipitable water (solid line). Dots are data points from Justice *et al.* (1991).

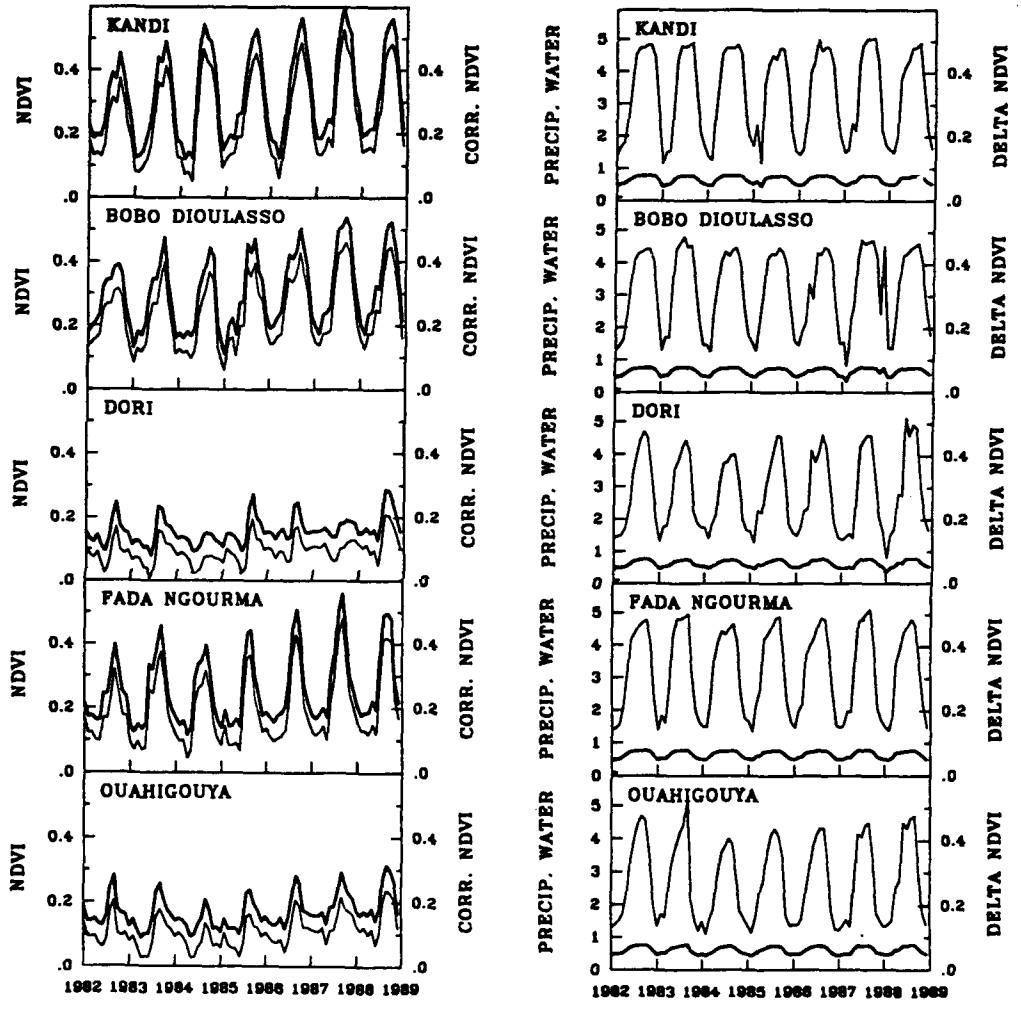

Figure 18: Plots of NDVI, corrected NDVI, precipitable water and delta NDVI. NDVI and precipitable water are thin solid lines while corrected NDVI and delta NDVI are thick solid lines

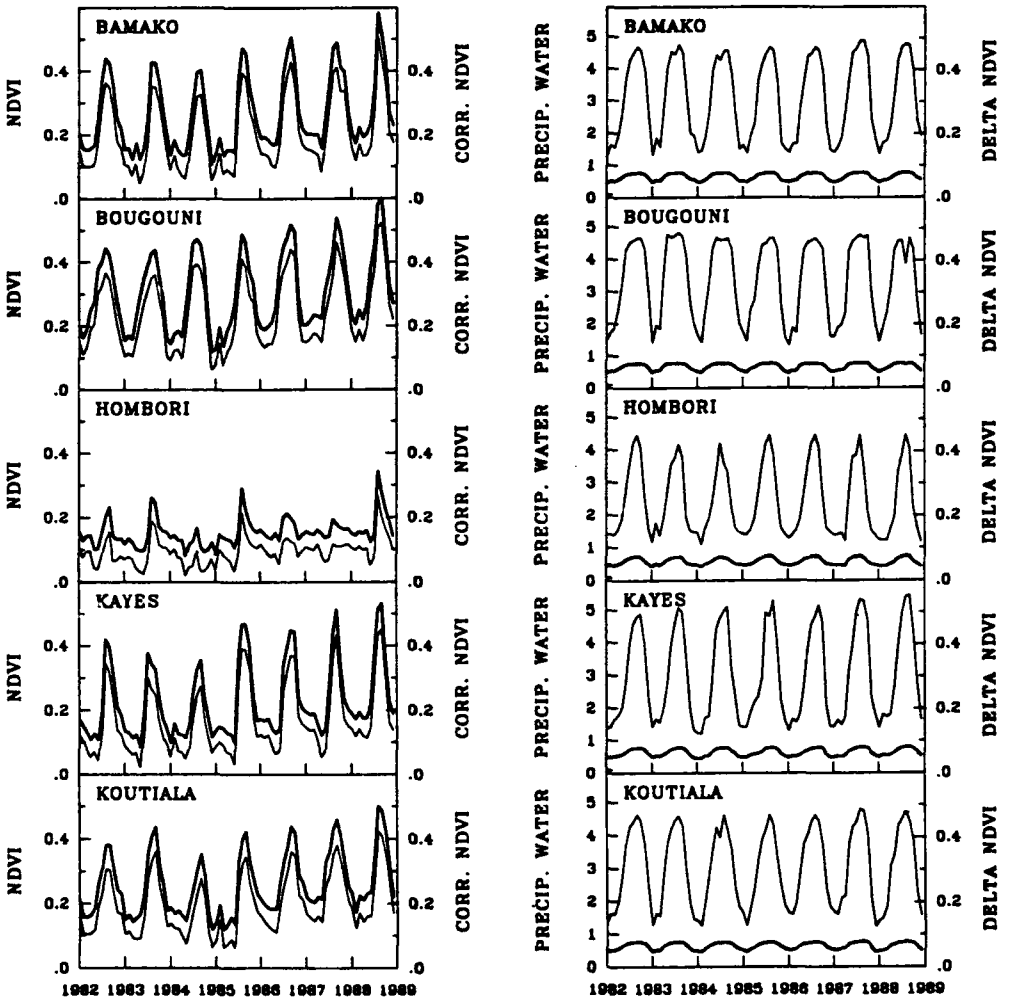

Figure 18: continued.

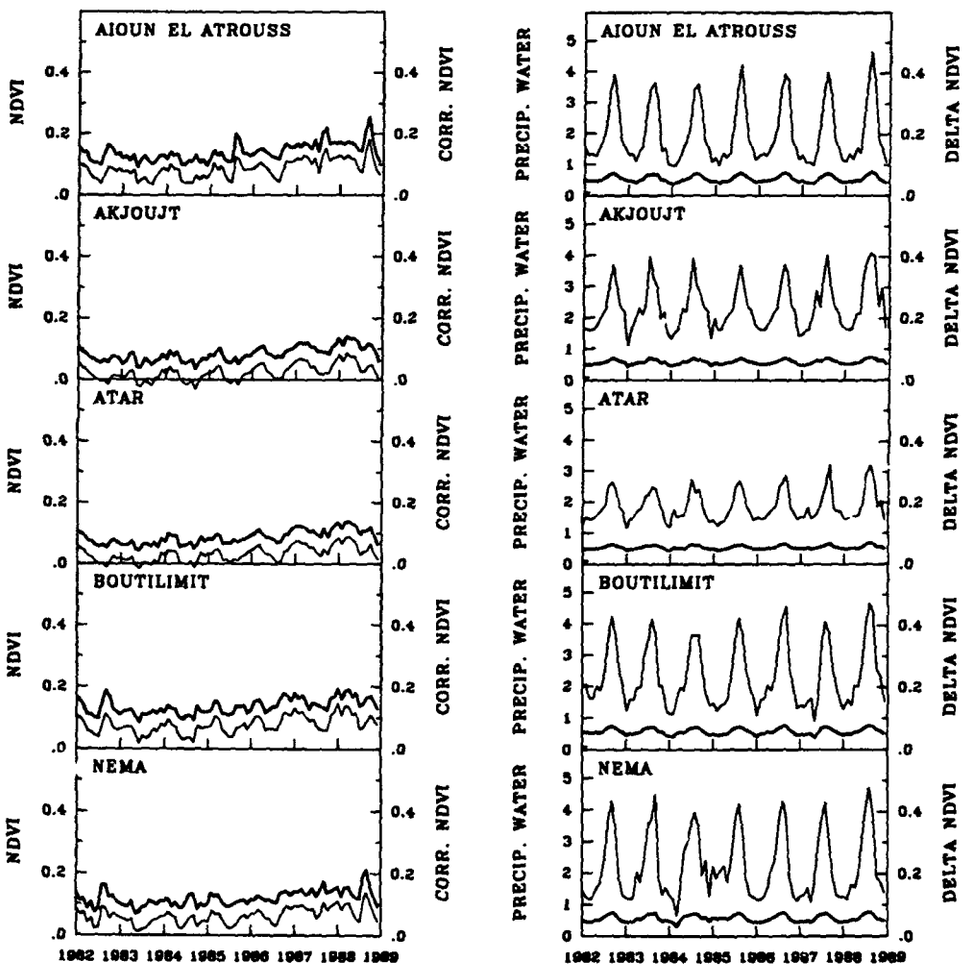

Figure 18: continued.

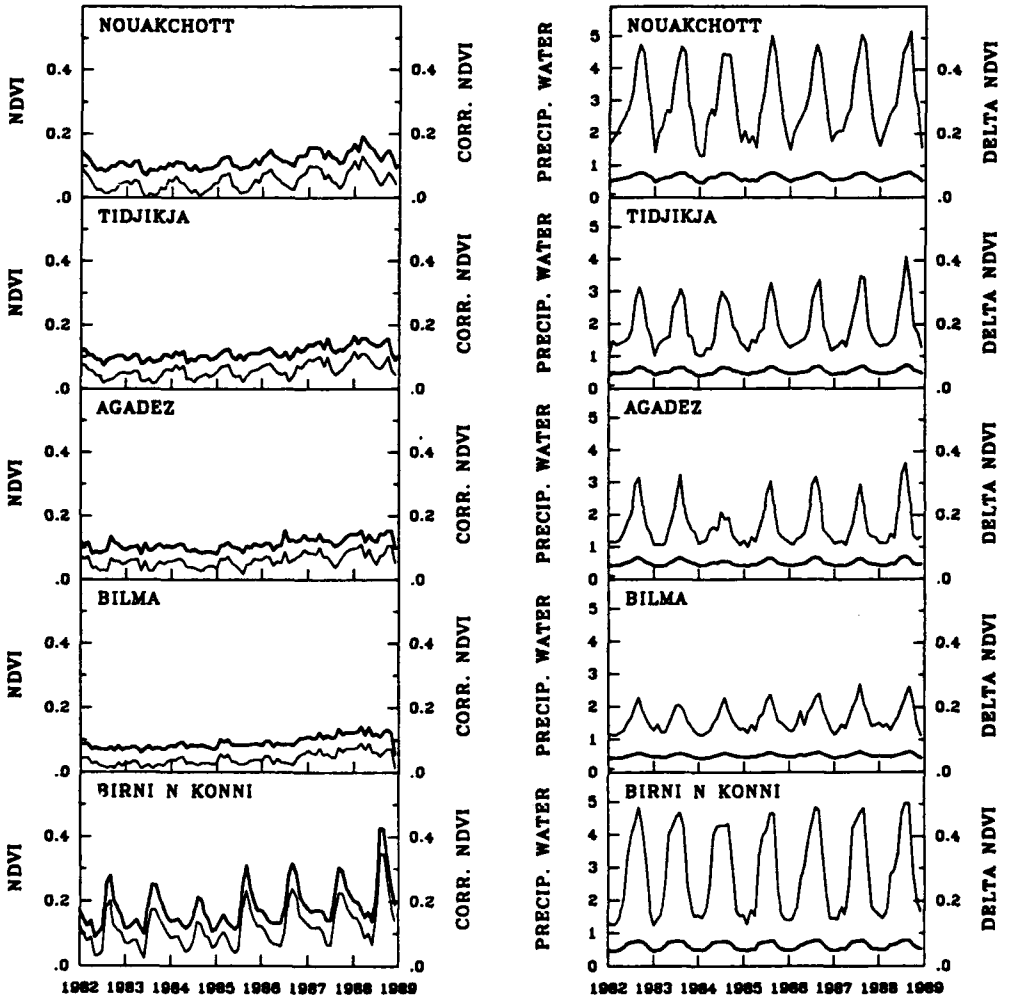

Figure 18: continued.

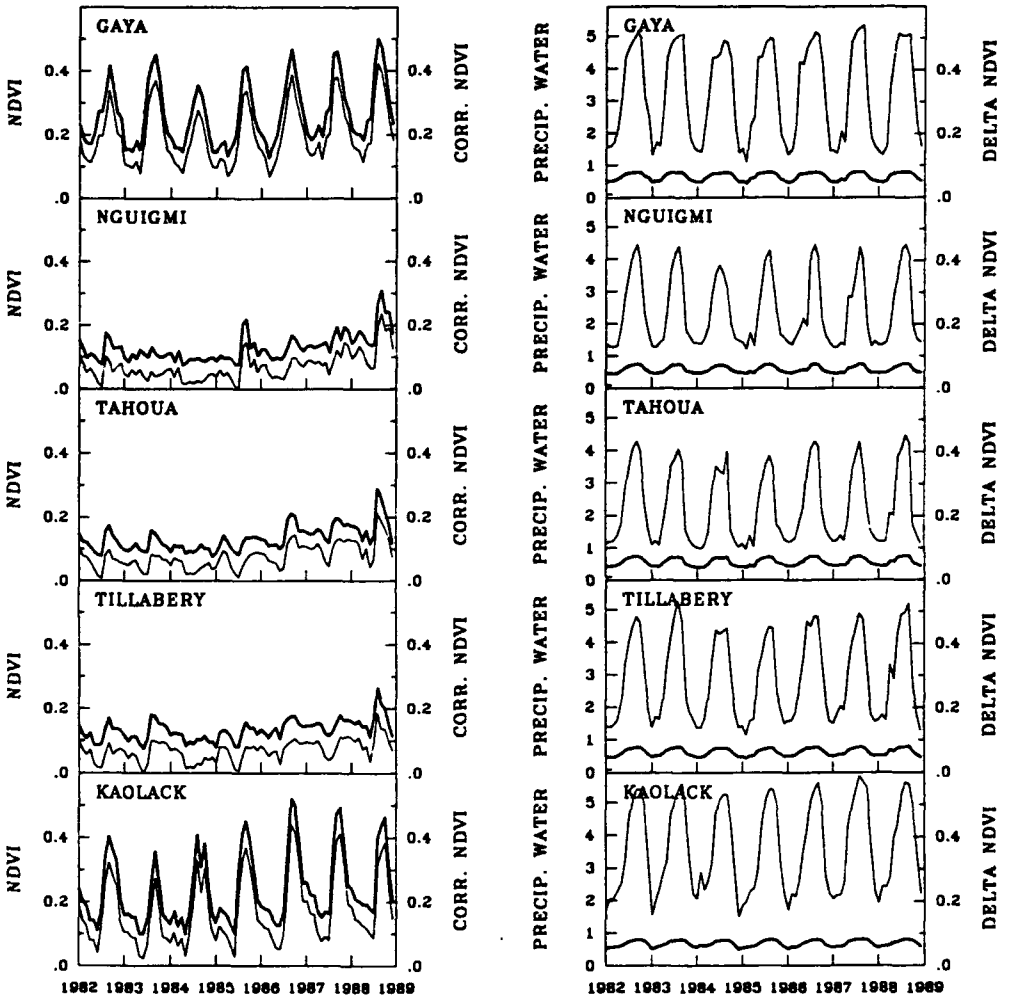

Figure 18: continued.

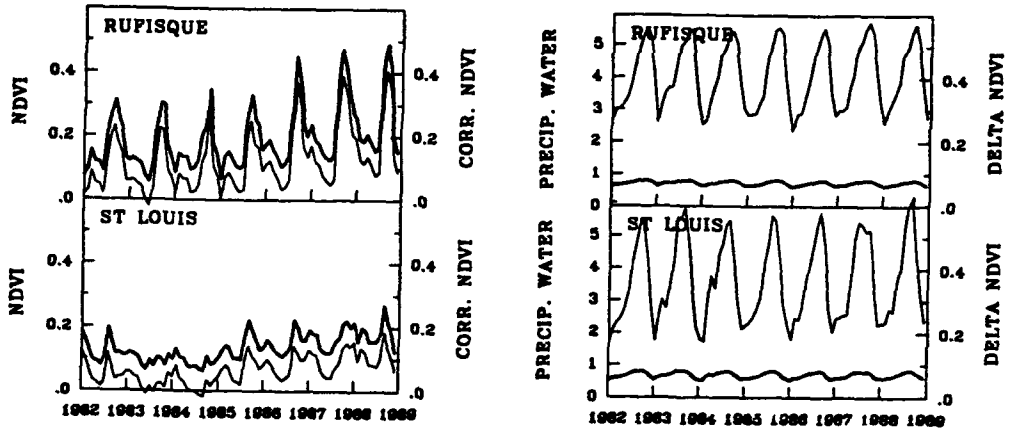

Figure 18: continued.

increase at Nema. On the other hand, the peak was reduced an average of 63% at N'Guigmi and 51% at Dori. Again, most reductions were closer to 20%.

May (Figure 19d) had the fewest occurrences of secondary peaks, and mixed results as far as peak reduction. Four stations experienced increased magnitudes, while three others experienced no change. At the same time, Akjoujt, whose peak magnitude was increased by 14% in February, now shows an average decrease of 57% for May. Since moisture is higher in May than in February, it is possible that the February peak is more related to aerosols, while the May peak is more closely linked to water vapor.

Figure 19e shows the overall reduction of the secondary peak for all months in all years. In this plot, four stations show increases in the secondary peak. The three stations in Senegal show only minor increases, while Nema in Mauritania shows a 17% increase. In fact, in

every month Nema showed an increase in the secondary peak after water vapor corrections were applied. Again, as Nema is in semi-desert grassland adjacent to the Sahara, it may be more affected by aerosols than water vapor.

As can be seen, with water vapor corrections ≈ 0.10 NDVI units, a correction for water vapor alone is not large enough to entirely explain the secondary peaks whose magnitudes are up to three time larger than the water vapor correction could produce. It is, therefore, very likely that water vapor effects must combine with other effects (aerosol, soil, etc.) to produce the peaks.

Another point of interest is the effect of water vapor corrections on annually integrated NDVI. Table 6 shows the average annual integrated NDVI for each station for corrected *and uncorrected* NDVI data *and the percent* increase of the corrected NDVI. In general, the percent increase for the corrected data increases from north to south. It is obvious from table 6 that desert or semi-desert locations are affected the most by the water vapor corrections. Especially affected is Akjoujt, where annual integrated NDVI increased 242%. Since an annual NDVI of 0.6 is generally considered the lower limit for vegetation growth (Justice and Hierneaux 1986), the correction scheme increases Akjoujt's annual NDVI from corresponding to no growth to what is commonly found for wooded grassland (for uncorrected data). This is unreasonable, since Akjoujt has wadi type vegetation, which is very sparse (White 1983) and could hardly be called a wooded or a grassland. The effects of the corrections appear to affect the desert regions where the annual cycle of water vapor has a large amplitude. This is especially true when the NDVI cycle is of low amplitude.

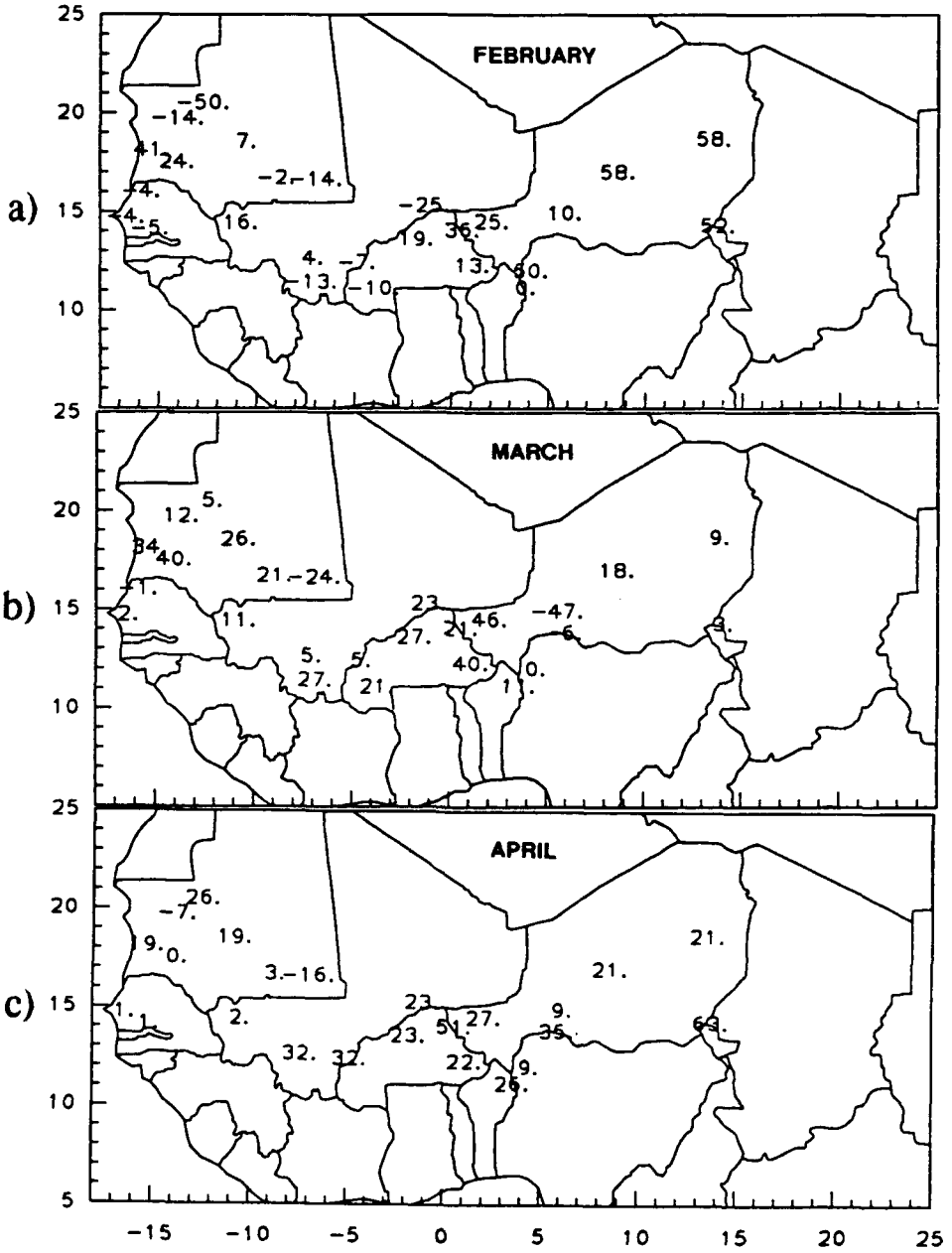

Figure 19: Average percent reduction of secondary NDVI peak for a) February, b) March, c) April, d) May, and e) all months.

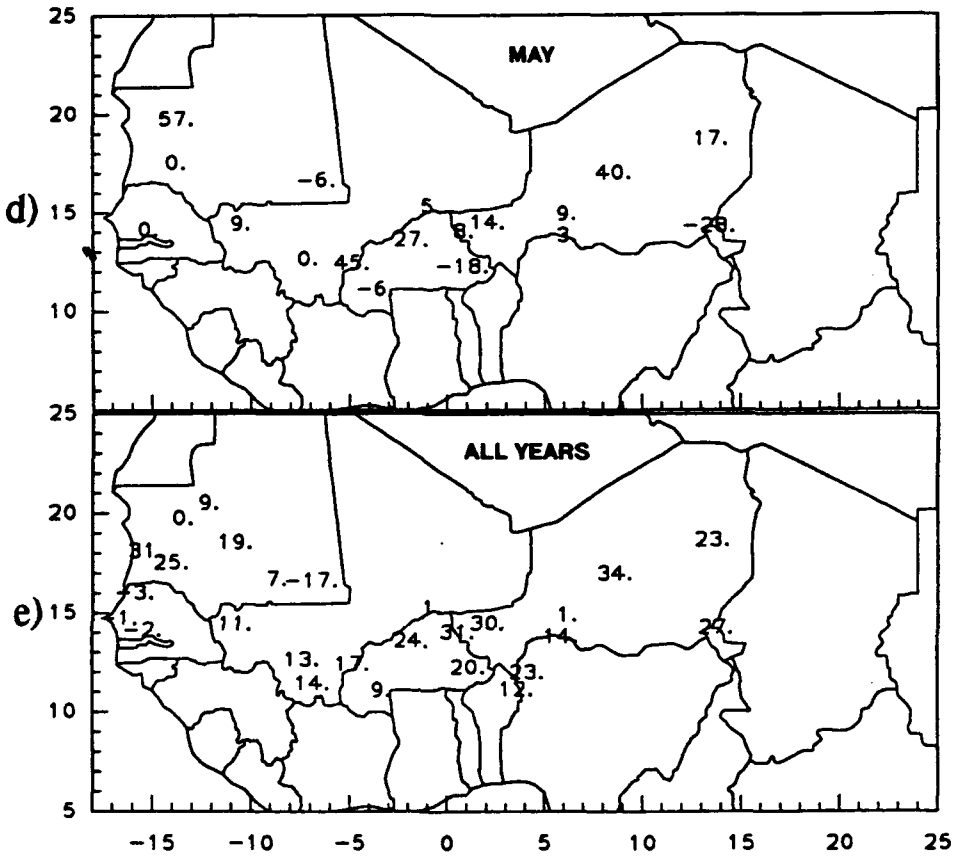

Figure 19: continued.

Table 6: Average Annual Integrated NDVI

Station	NDVI	Corrected NDVI	% Increase
Sudanian Woodland	2.779	3.590	28
Kandi	3.076	3.875	26
Bamako	2.424	3.203	32
Bougouni	2.896	3.702	28
Undifferentiated Woodland	1.902	2.696	42
Bobo Dioulasso	2.864	3.656	28
Fada NGourma	2.334	3.125	34
Ouahigouya	1.311	2.050	56
Kayes	1.994	2.758	38
Koutiala	2.349	3.125	33
Birni N Konni	1.445	2.195	52
Gaya	2.398	3.186	33
Kaolack	2.051	2.881	40
Rufisque	1.483	2.359	59
St. Louis	0.794	1.629	105
Sahel Acacia Wooded Grassland/Shrubland	1.009	1.722	71
Hombori	1.138	1.850	63
Dori	1.137	1.892	66
Aioun ElAtrous	1.027	1.687	64
Tahoua	0.912	1.593	75
Tillabery	0.830	1.588	91
Northern Sahel Semidesert	0.692	1.354	96
Atar	0.371	1.025	176
Boutilimit	0.927	1.631	76
Nema	0.748	1.431	91
Tidjikja	0.703	1.357	93
Agadez	0.712	1.328	87

Table 6: continued.

Station	NDVI	Corrected NDVI	% Increase
Wadis			
Akjoujt	0.284	1.000	252
Atlantic Coastal Desert			
Nouakchott	0.619	1.397	126
Absolute Desert			
Bilma	0.486	1.103	148
Swamp/Aquatic Vegetation			
N'Guigmi	0.849	1.554	83

5.2 Corrections of NDVI for Aerosols

Corrections of NDVI were made for aerosols based on data calculated by Holben *et al.* (1991). They modeled the effects of aerosols on the NDVI signal at the satellite level. They used the radiative transfer code of Ahmad and Fraser (1982) with Saharan type aerosols (index of refraction of aerosols = 1.55 - 0.0035i). They calculated $\Delta NDVI$ for a nominal NDVI reflectance of .20 in the near infrared and .15 in the visible giving an NDVI of .142. $\Delta NDVI$ will vary with different NDVI values because of changes of reflectances in each channel. Individual channel reflectances were not available for this study, but since a NDVI of .142 is near the values of our NDVI and since this is the only data from a model using Saharan sized aerosols, it was the best choice.

Holben *et al.* (1991) calculated $\Delta NDVI$ for various τ_a (0.2 to 1.0) and for the backscatter, forward scatter and nadir viewing angles. The present study used the nadir viewing angle data since the maximum value compositing technique (Holben 1986) should choose

NDVI from near nadir viewing angles. A linear regression was applied to the Holben *et al.* data. The regression equation is:

$$\Delta NDVI = 0.012 - 0.029\tau_a \tag{9}$$

where $\Delta NDVI$ is the change in NDVI and τ_a is the aerosol optical depth (thickness). A plot of the regression line is shown in Figure 20.

The data from the Ben Mohamed *et al.* (unpublished manuscript) study's seven Nigerian stations were then used to calculate $\Delta NDVI$ for the NDVI values of these stations. Figure 21 shows time series for these station's NDVI, corrected NDVI, $\Delta NDVI$ and τ_a. Examining these series, it can be seen that all stations experienced a secondary peak in April of 1987 and that three stations experienced peaks in May 1986. After corrections for aerosols were applied, analysis revealed 60% of the peaks were reduced slightly; however, the other 40% of the peaks were increased (Table 7). In addition, two stations (Tahoua and Zinder) which had no peaks, now had peaks in May of 1986.

Table 7: Effects On Secondary Peaks by Aerosol Corrections

Station	May 1986 Peak Magnitude Uncorrected/Corrected	April 1987 Peak Magnitude Uncorrected/Corrected	% Reduction 1986/1987
Agadez	.010/.0155	.028/.0205	-55/27
Bilma	.017/.0165	.023/.0215	3/7
Birni N Konni	*	.010/.0145	*/-45
N Guigmi	.006/.0045	.011/.010	25/9
Niamey	No peaks	.017/.020	NA/-18
Tahoua	No peak/.017	.017/.0165	-100/3
Zinder	No peak/.008	.028/.032	-100/-14

* Insufficient data

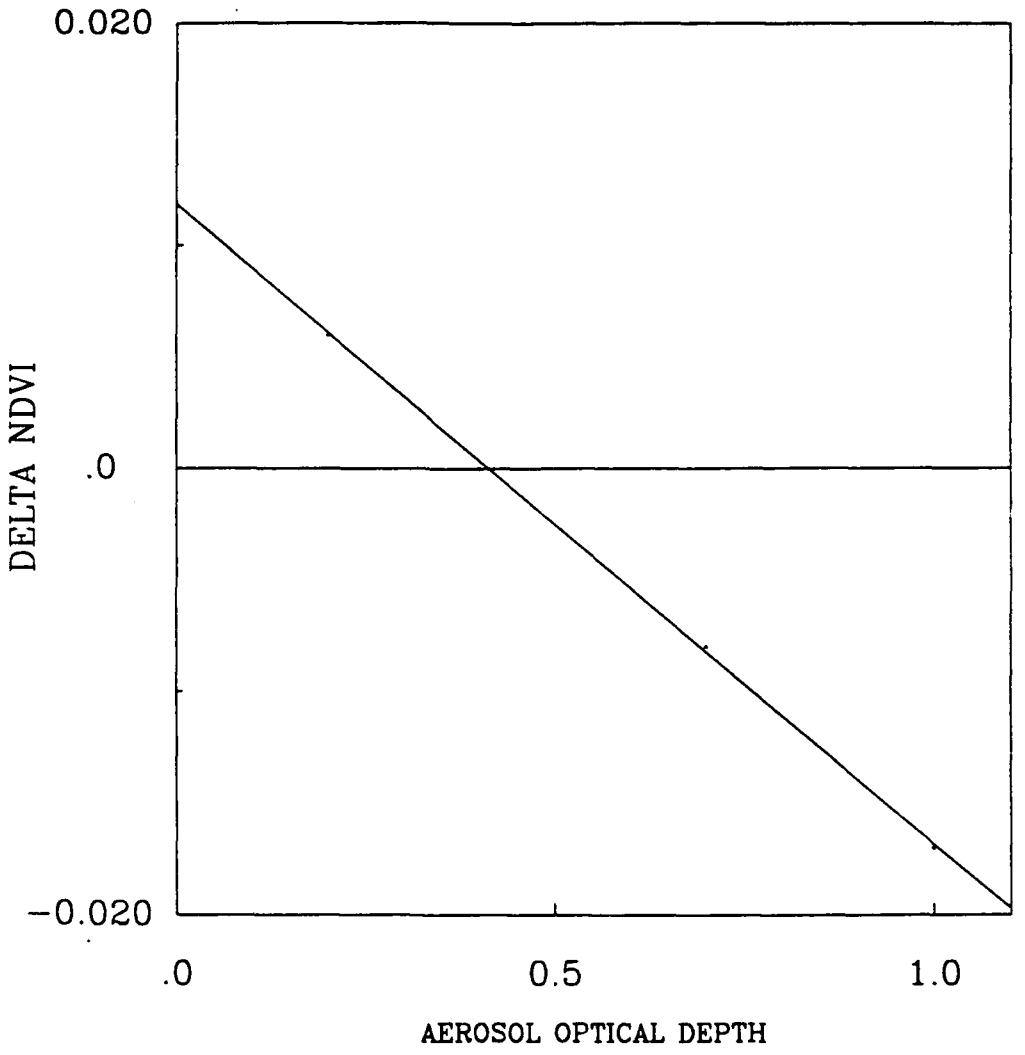

Figure 20: Plot of the regression of delta NDVI with aerosol optical depth (solid line). Small dots are data points from Holben *et al.* 1991.

Once again, differences in what constitutes a monthly value are a likely cause of the problems seen in the results of aerosol corrections. If aerosol data were available for the specific date when the reflectances for the NDVI were measured, corrections for aerosols might have produced better results. The aerosol corrections were on the order of the magnitude of the peaks in these cases (≈ 0.01), however, for some stations shown in section 3.1, the magnitude of the peaks was much larger and could not be explained by aerosol effects. If fact, with both water vapor and aerosol corrections, numerous secondary NDVI peaks would still exceed the corrections for both of these parameters. It is then highly likely that secondary NDVI peaks are a result of the interactions of all the influences on NDVI, and not just water vapor and aerosols.

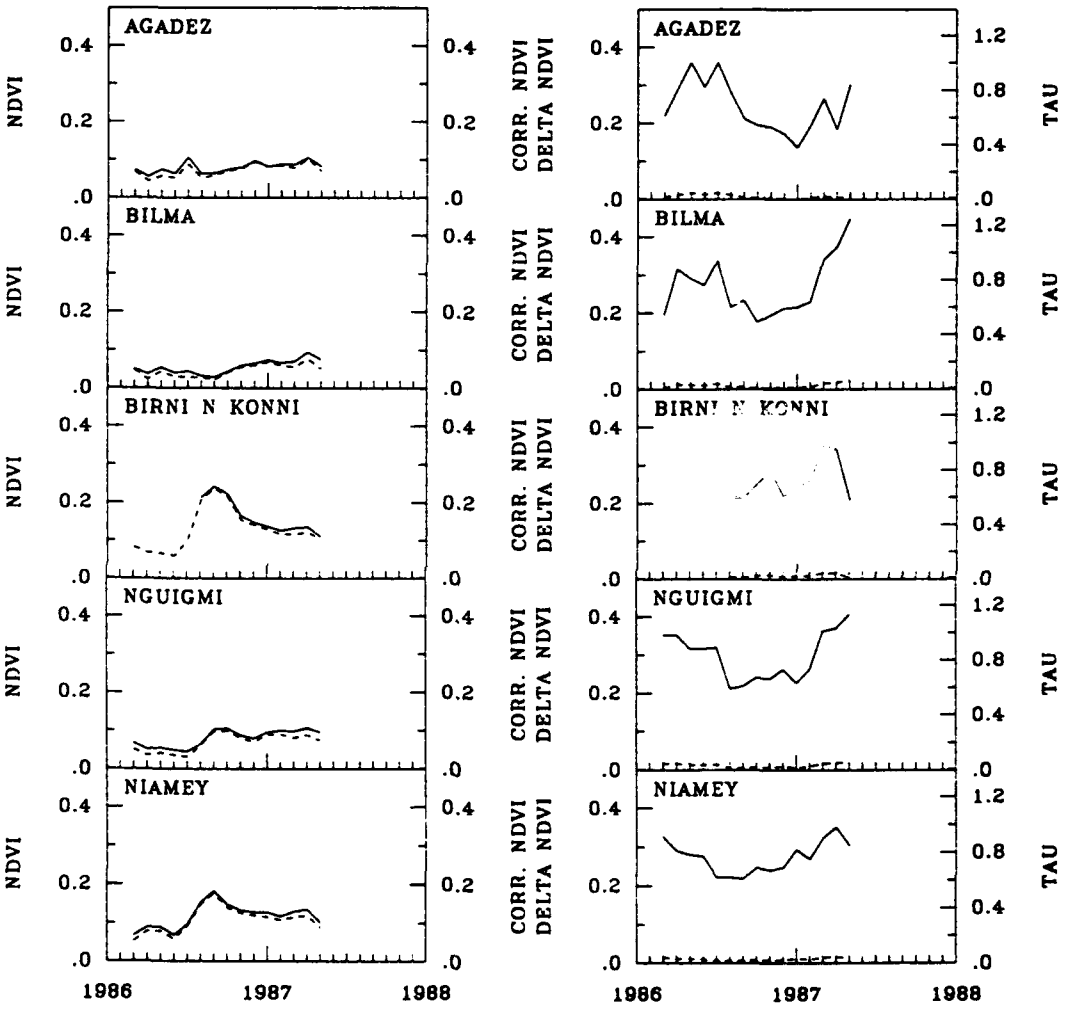

Figure 21: Plots of NDVI, corrected NDVI, delta NDVI and aerosol optical thickness (tau). NDVI and delta NDVI are dashed lines, while corrected NDVI and tau are solid lines.

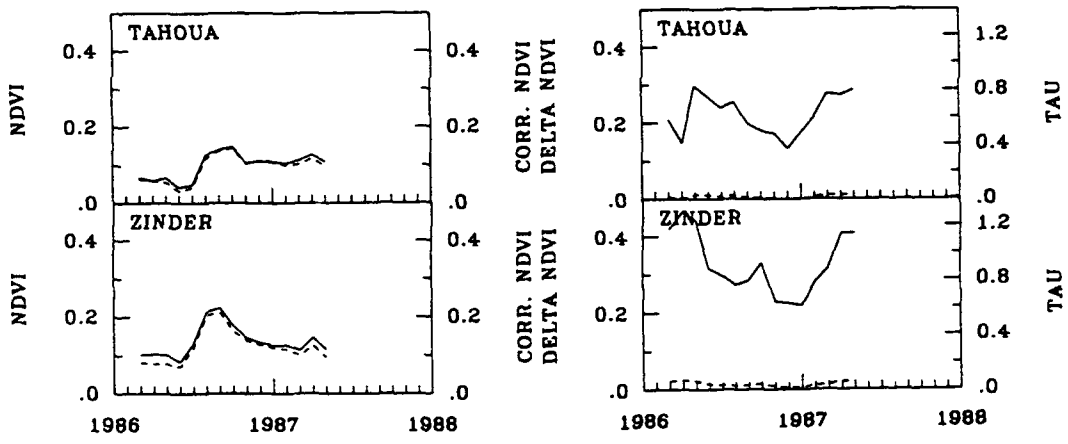

Figure 21: continued.

Chapter 6

NDVI-Rainfall Correlations: Corrected vs. Uncorrected NDVI Data

Several authors (Davenport and Nicholson 1991, Malo and Nicholson 1990) have attempted to examine NDVI-rainfall relationships using lagged linear correlation. In a further attempt at evaluating the effects of water vapor corrections, lagged linear correlations were computed for stations in this study. In the case of the water vapor corrected NDVI data, enough data were available to study the results by vegetation formation (from White's 1983 memoir) as well as by station. For aerosols, the short length of the aerosol record did not provide for a sufficient number of months with rainfall for correlation coefficients to be calculated.

6.1 NDVI-Rainfall Correlations for Water Vapor Corrected NDVI data

Using the same technique employed by Malo and Nicholson (1990), Pearson's correlation coefficient was computed for 24 of the 27 station data set. Three of the 27 stations, all in Senegal, had incomplete rainfall records and were eliminated. Correlations were computed between monthly NDVI and monthly rainfall only for months when rainfall exceeded 10mm. This was done to avoid the skewing of the rainfall data caused by many months of no rainfall. Correlations were calculated at lags of zero months (i.e., the concurrent month), the previous month, the two previous months and the concurrent plus two previous months.

Table 8 shows a breakdown of all 24 stations into their respective vegetation classifications. Left hand values in each column represent NDVI- rainfall correlations for uncorrected NDVI data. The right hand values correspond to NDVI-rainfall correlations for the corrected data.

For Sudanian Woodland, the highest correlations were for the concurrent plus two previous months. The overall vegetation type correlation was not improved by the water vapor corrections. This is true for the individual stations as well. The reason for this has to do with the phase or timing of water vapor maxima, the phase of the rainfall and the amplitudes of the NDVI and water vapor cycles. In this situation, water vapor and rainfall are in phase; that is, maximum rainfall usually occurs during the month of maximum water vapor (or precipitable water). The NDVI and water vapor have similar amplitudes in their seasonal cycles(See Figure 5). Because of this, corrected NDVI has almost the same amplitude

as uncorrected NDVI, but every value is simply larger. When correlations are calculated, they are the same because deviations from the mean in each NDVI case are nearly the same.

The Undifferentiated Sudanian Woodland had different results. In this case, correlations for corrected data were slightly higher in all but one case. Statistically, the differences between corrected and uncorrected NDVI-rainfall correlations are insignificant. There are reasons for the different correlation coefficients. The phase of the water vapor, rain and amplitude of the NDVI and water vapor cycles again are the causes, but for different reasons. In this vegetation formation, water vapor and rainfall are all in phase; however, NDVI has a smaller seasonal amplitude than water vapor. Thus water vapor corrections for NDVI produced higher NDVI values in the rainy season, which resulted in slightly higher correlations coefficients.

The one exception was Gaya. It turns out that for the time period 1982 to 1988, water vapor and rainfall were often out of phase at Gaya, even though water vapor and NDVI had similar magnitudes. So for this case, NDVI's phase relationship with rainfall was altered by the water vapor corrections and the correlation dropped somewhat. The corrections did, however, bring Fada N'Gourma in line with the rest of the stations in that vegetation formation.

Sahel Acacia wooded grassland or shrubland had the best correlation with the previous two months. Tahoua had the largest increase in corrected NDVI correlation, but again, it was not statistically significant. At Tahoua, rainfall and water vapor are in phase and water vapor has a much larger amplitude than NDVI. So at Tahoua, NDVI is much higher when corrected, thus producing a higher correlation coefficient.

The desert formations had varying results when correlated. Nouakchott had very poor correlations for every time lag while insufficient rain fell at Bilma to do any correlations. Akjoujt, in a Wadi type vegetation formation, was different. Akjoujt correlated best with NDVI and rainfall in the same month. This makes sense, since in a wadi (a normally dry streambed), rainfall is concentrated. The vegetation then responds quickly to the limited water supply, which will soon be unavailable. As to why the corrected NDVI correlation is lower, the answer is because rainfall and water vapor are out of phase. In most cases, sufficient rainfall fell in only one month of the year, but water vapor maximums were always in a different month. When water vapor corrections were made, they increased NDVI the most in a month other than the month the rain fell. Corrections in this case put NDVI and rainfall out of phase and the correlation fell.

Finally, N'Guigmi, a station in a swamp and aquatic vegetation formation, showed best correlations for the concurrent plus two previous months. Corrected NDVI resulted in higher correlation coefficients, but were statistically equivalent to uncorrected correlation coefficients. Water vapor and rainfall were in phase and NDVI had a smaller amplitude than water vapor.

In many cases the water vapor correction to NDVI produced larger NDVI- rainfall correlation coefficients. None of the corrected NDVI-rainfall correlations were found to be statistically different from uncorrected NDVI-rainfall correlations. It should be noted again that these monthly data are not the same types of monthly data. However, one should expect that, once water vapor data are available for the specific dates monthly NDVI was retrieved, corrected NDVI based on that water vapor data will not have significantly

improved NDVI-rainfall correlations.

Table 8: NDVI-Rainfall Correlations for Uncorrected/Corrected Data

Station	0	1	0+1	1+2	0+1+2
Sudanian Woodland	.586/.591	.788/.789	.795/.799	.795/.791	**.844/.844**
Kandi	.523/.528	.789/.790	.775/.779	.815/.813	**.848/.848**
Bamako	.759/.765	.899/.900	.920/.924	.855/.855	**.938/.939**
Bougouni	.585/.589	.808/.808	.836/.838	.834/.833	**.892/.892**
Undifferentiated Woodland	.479/.488	.733/.737	.733/.739	.769/.771	**.808/.813**
Bobo Dioulasso	.522/.565	.770/.772	.762/.770	.752/.750	**.794/.798**
Fada N'Gourma	.390/.402	.746/.750	.712/.721	**.816**/.818	.815/**.822**
Ouahigouya	.404/.421	.762/.770	.699/.713	.818/.825	**.821/.834**
Kayes	.470/.476	.768/.765	.839/.842	.761/.759	**.869/.870**
Koutiala	.543/.558	.882/.884	.828/.838	.879/.873	**.937/.939**
Birni N Konni	.368/.374	.786/.795	.794/.803	.891/.897	**.912/.919**
Gaya	.461/ 545	.711/.705	.744/.736	.787/.782	**.821/.814**
Sahel Acacia Wooded Grassland/Shrubland	.037/.048	.665/.686	.080/.092	**.686/.703**	.104/.116
Dori	.420/.444	.818/.827	.811/.832	.826/.840	**.863/.887**
Hombori	.366/.373	.713/.714	.783/.788	.756/.755	**.834/.836**
Aioun ElAtrous	-.328/-.231	**.564/.590**	.299/.381	.509/.509	.447/.448
Tahoua	.478/.506	.697/.714	**.765/.793**	.704/.719	.763/.787
Tillabery	.332/.363	.708/.737	.646/.684	**.734**/.747	.726/**.752**
Northern Sahel Semidesert Grass/Shrubland	.205/.265	.496/.534	.480/.547	.548/.554	**.561/.597**
Atar	-.213/-.174	-.046/.031	-.154/-.084	-.063/.003	-.161/-.096
Boutilimit	.277/.342	.706/.730	.619/.680	**.737**/.713	.707/**.735**
Nema	.355/.408	.545/.594	.627/.697	.590/.586	**.686/.708**
Tidjikja	.013/.236	.511/.542	.435/.544	**.552/.580**	.466/.567
Agadez	-.166/-.064	.199/.309	.019/.183	**.359/.432**	.225/.348

Table 8: continued.

Station	0	1	0+1	1+2	0+1+2
Wadis					
Akjoujt	**.749/.720**	-.116/-.106	.483/.467	-.039/-.025	.490/.478
Atlantic Coastal Desert					
Nouakchott	.001/.135	**.101/.208**	.057/.193	.079/.168	.048/.174
Absolute Desert					
Bilma	*/*	*/*	*/*	*/*	*/*
Swamp/Aquatic Vegetation					
N'Guigmi	.333/.362	.669/.683	.709/.737	.689/.699	**.760/.783**
Totals (Stations)	1/1	2/2	1/1	5/2	13/16

* Insufficient data

Chapter 7

Summary and Conclusions

The purpose of this study was to: examine the spatial and temporal patterns of water vapor, aerosols and the secondary peak in the NDVI; examine the relationships between NDVI and water vapor; correct NDVI for the effects of water vapor and aerosols in an attempt to eliminate or reduce the secondary peak and to examine the effect of corrections on annually integrated NDVI and NDVI-rainfall correlations.

Contoured maps were used to display the spatial and temporal patterns of water vapor; while time series were used in the case of aerosols. A vector format was implemented to display the magnitude and phase of the secondary NDVI peak. The vectors showed some interesting patterns. In some years, the secondary peaks were "clustered" together in a particular month. In other years, the secondary peaks tended to occur mostly in the same month across the entire region.

Examining individual maps of water vapor could not show a clear relationship between water vapor and the secondary peak. It was found that, at times, the secondary peak

occurred in areas with water vapor below the seven year average. At other times, the peaks occurred in regions where above average water vapor was found. These results point to the difficulties presented by data differences. Monthly water vapor and aerosol data were averages of the daily values. Monthly NDVI, however, is designed to represent peak photosynthetic activity (Tucker and Sellers 1986) and thus is the highest value of NDVI for the month. It is probable that having specific dates for the NDVI measurements and data for that date for water vapor and aerosols would yield more conclusive results.

An effort was made to examine more closely the relationships between NDVI and water vapor using Pearson's correlation coefficient. The correlations were done between water vapor and NDVI anomalies found after removing the monthly means. The year was divided into four seasons: two transition seasons and a wet and dry season. Dry season NDVI-water vapor correlations were poor. During the dry season, little photosynthetic activity occurs, so the NDVI signal would remain constant. However, at this time of the year, effects of water vapor are at their lowest, and the effects of illumination geometry, soil and aerosols may approach the magnitude of the water vapor influence. In that way, the competing effects produce low correlations. Correlations were also done using running means of NDVI and water vapor anomalies. These correlations tended to show the out of phase relationship between NDVI and water vapor. This shows that as water vapor increases, NDVI decreases, which theory suggests.

The transition to the wet season was different. Now, several stations had negative correlations. At this time, rainfall was limited, but water vapor steadily increased. Without the rain, vegetation does not grow so NDVI should remain steady. However, increased water

vapor attenuates the NDVI signal, so as water vapor increases, its influence on NDVI begins to exceed the other factors on the NDVI. Thus, increased water vapor NDVI decreases the NDVI and the correlations are negative.Correlation for the other seasons described as well as annually were all very low. It appears that water vapor induced fluctuations in NDVI were only strong enough in the transition to wet season.

Corrections of NDVI for water vapor were made. Changes in NDVI due to precipitable water (as inferred by surface water vapor) were calculated using a regression equation. The regression equation itself was developed from the results of a radiative transfer model published by Justice *et al.* (1991). After the NDVI had been corrected for water vapor, it was examined for the effect on the secondary peak. In most cases, the secondary peak had been reduced. However, few stations experienced increases in either the number or magnitude of secondary peaks. Annual integrated NDVI, a measure of gross productivity (Tucker and Sellers 1986) was increased by the water vapor corrections. In some cases, annually integrated NDVI was increased by 252%, which was unrealistic for that particular desert location.

Another correction to NDVI was made, this time for the effects of aerosols. The change in NDVI due to aerosols was determined using a regression equation relating ΔNDVI to τ_a. The regression equation was formulated from data calculated by a radiative transfer model which included Saharan sized aerosols. Again, the effects on secondary peaks were examined. It was found that 60% of the peaks were reduced. However, new peaks were created at two stations and 40% of the peaks were increased.

In the case of water vapor corrections, a maximum correction of about 0.10 was made.

The correction for aerosols was at most about 0.02. In view of the fact that many of the secondary peaks in the NDVI signal are larger than 0.12 (the correction for both water vapor and aerosols), it is clear that more than water vapor and aerosols are responsible for producing the secondary NDVI peaks. Even if water vapor and aerosol data were available for the date the NDVI was measured, the corrections for their effects would not be large enough to eliminate the peaks.

In another examination of the effects of the corrections, correlations of NDVI with rainfall were done with uncorrected and corrected NDVI data. Correlations were done only for water vapor corrected data as the time period of aerosol corrected data did not include a sufficient number of month with rain. Corrected data often improved NDVI-rainfall correlations, but not always. It was found that the phase of water vapor with respect to rainfall, and the amplitude of the seasonal cycle of NDVI with respect to that of water vapor were important. Although the corrected NDVI often produced larger correlation coefficients, they were not statistically significant differences.

7.1 Recommendations for Future Study

As mentioned throughout this study, there were differences between the meaning of the word *monthly* with respect to water vapor, aerosols and NDVI. The specific dates that the monthly NDVI values are obtained are needed so that the NDVI could be analyzed with the same day's water vapor or aerosol data. When corrections for water vapor and aerosol are applied using these types of data, the NDVI curve should look much smoother, although it

is apparent that this will not eliminate secondary peaks. Still, such corrections should lead to improved estimates of primary production, and may allow estimates in regions which were initially thought to have to little vegetation.

In addition to the problem of differing time frames, there is a serious lack of available aerosol data from which NDVI corrections could be made. At present, a network of sun photometers has been set up in West Africa and is monitor aerosol as well as water vapor (Holben *et al.* 1991). When longer aerosol data sets are available, they should prove useful.

Another important point is that the corrections for NDVI in this study were based on the only model results available. In the future, a better understanding of aerosols and water vapor in the Sahelian region may produce corrections for NDVI which can eliminate secondary peaks and provide more accurate estimate of vegetation growth.

Using sun photometers or station's water vapor pressure or even radiosonde data for aerosols and water vapor still present limitations: they are all limited in space. While water vapor may be extrapolated from individual stations with some confidence (provided stations are not too widely separated), Holben *et al.* (1991) has shown that aerosols vary so much in time and space that extrapolation from a point is not very reliable. Tanre and Legrand (1990) have developed techniques for determining aerosol optical thickness over land using satellites. Justice *et al.* (1991) has suggested satellite retrieval of precipitable water also. While both of these methods require further work, they show promise and would give the best spatial and temporal coverage of data available.

With the intense interest in monitoring vegetation using satellites, it is important that research continue towards operational corrections of NDVI for atmospheric effects. Once

these corrections have been perfected, NDVI should provide a much better estimate of what the vegetation is actually doing.

References

Ahmad, Z., and Fraser, R.S., 1982: An iterative radiative transfer code for ocean-atmosphere system. *J. Atmos. Sci.*, **39**, 656-665.

Ben Mohamed, A., and Frangi, J.-P., 1983: Humidity and turbidity parameters in Sahel: A case study for Niamey (Niger). *J. Clim. Appl. Meteor.*, **22**, 1820-1823.

Ben Mohamed, A., and Frangi, J.-P., 1986: Results from ground-based monitoring of spectral aerosol optical thickness and horizontal extinction: Some specific characteristics of dusty Sahelian atmospheres. *J. Clim. Appl. Meteor.*, **25**, 1807-1815.

Ben Mohamed, A., Frangi, J.-P., Fontan, J., and Druilhet, A., 1992: Spatial and temporal variations of atmospheric turbidity and related parameters in Niger. Submitted to *J. Appl. Meteor.*

Braslau, N., and Dave, J.V., 1973: Effects of aerosols on the transfer of solar energy through realistic model atmospheres. Part I: Non-absorbing aerosols. *J. Appl. Meteor.*, **12**, 601-615.

Cerf, A., 1980: Atmospheric turbidity over West Africa. *Contibutions to Atmospheric Physics*, **53**, 414-429

D'Almeida, G.A., 1987: On the variability of desert aerosol radiative characteristics. *J. Geophys. Res.*, **92**, 3017-3026.

Davenport, M.L., and Nicholson, S.E., 1991: On the relationship between rainfall and the Normalized Difference Vegetation Index for diverse vegetaion types in East Africa. *Int. J. Remote Sens.* (in press).

Dubief, J., 1979: Review of the North African climate with particular emphasis on the production eolian dust in the Sahel zone and in the Sahara. *Saharan Dust*, SCOPE 14, C. Morales, Ed., Wiley, New York, 27-48.

Eck, T.F., and Kalb, V.L., 1991: Cloud-screening for Africa using a geographically and seasonally variable infrared threshold. *Int. J. Remote Sens.* **12**, 1205-1221.

FAO/UNESCO, 1977: *Soil Map of the World. Vol. VI, Africa.* UNESCO, Paris.

Farquart, Y., Bonnel, B., Chaoui Roquai, M., Sauter, R., and Cerf, A., 1987: Observations of Saharan aerosols: Results of ECLATS field experiment. Part I: Optical thickness and aerosol size distributions. *J. Clim. Appl. Meteor.*, **26**, 28-37.

Hayward, D.F., and Oguntoyinbo, J.S., 1987: *The Climatology of West Africa*, Barnes and Noble Books, Totowa, New Jersey, 271pp.

Holben, B.N., 1986: Characteristics of maximum-value composite images from temporal AVHRR data. *Int. J. Remote Sens.* **7**, 1417-1434.

Holben, B.N., Eck, T.F., and Fraser, R.S., 1991: Temporal and spatial variability of aerosol optical depth in the Sahel region in relation to remote sensing. *Int. J. Remote Sens.*, **12**, 1147-1163.

Huete, A.R., Jackson, R.D., and Post, D.F., 1985: Spetral response of a plant canopy with different soil backgrounds. *Remote Sens. Environ.*, **17**, 37-53.

Huete, A.R., Tucker, C.J., 1991: Investigation of soil influences in AVHRR red and near-infrared vegetation index imagery. *Int. J. Remote Sens.* **12**, 1223-1242.

Junge, C.E., 1963: *Air Chemistry and Radioactivity.* Academic Press, 382pp.

Justice, C.O., and Hiernaux, P.H.Y., 1986: Monitoring the grasslands of the Sahel using NOAA AVHRR data: Niger 1983. *Int. J. Remote Sens.* **7**, 1475-1497.

Justice, C.O., Townshend, J.R.G., Holben, B.N., and Tucker, C.J., 1985: Analysis of the phenology of global vegetation using meteorological satellite data. *Int. J. Remote Sens.*, **6**, 1271-1318.

Kalu, A.E., 1979: The African Dust Plume: its characteristics and propagation across West Africa in winter. *Saharan Dust,* SCOPE 14, C. Morales, Ed., Wiley, New York, 95-118.

Lare, A.R., 1992: An investigation into land surface feedback and the African drought using climatonomy modeling. Unpublished Ph.D. dissertation, Florida State Univ., pp.

Malo, A.R., and Nicholson, S.E., 1990: A study of rainfall and vegetation dynamics in the African Sahel using Normalized Difference Vegetation Index. *J. Arid Environ.*, **19**, 1-24.

Monthly Climatic Data for the World, 1982- 1988. National Oceanic and Atmospheric Administration/National Enviromental Satellite, Data and Information Service/National Climatic Data Center, Ashville, North Carolina.

Nicholson, S.E., 1989: African drought: Characteristics, causal theories, and global teleconnections. *Symposium on Contributions of Geophysical Sciences to Climate Change,* Vancouver, British Columbia, 79-100.

Nicholson, S.E., Davenport, M.L., and Malo, A.R., 1990: A comparison of vegetation response to rainfall in the Sahel and East Africa using Normalized Difference Vegetation Index from NOAA. *Clim. Change,* **17,** 209-241.

Nicholson, S.E., Kim, J., and Hoopingarner, J., 1988: Atlas of African rainfall and its interannual variability. Dept. of Meteor., Florida State Univ., Tallahassee, Florida, 237pp.

Oluwafemi, C.O., 1979: Preliminary solar spectrophotometric measurements of aerosol optical density at Lagos, Nigeria, *Atmos. Environ.* **13,** 1611-1615.

Pendorf, R., 1957: Tables of refractive index for standard air and the Rayleigh scattering coefficient for the spectral region between 0.2 and 20.0μm and their application to atmospheric optics. *J. Opt. Soc. Amer.,* **47,** 176-182.

Sellers, P.J., 1985: Canopy reflectance, photosynthesis and transpiration. *Int. J. Remote Sens.,* **6,** 1335-1372.

Tanre, D., and Legrand, D., 1991: On the satellite retrieval of Saharan dust optical thickness over land: Two different approaches. *J. Geophys. Res.,* **96,** 5221-5227.

Tucker, C.J., and Miller, L.D., 1977: Contribution of the soil spectra to grass canopy spectral reflectance. *Photogrammetry Engineering and Remote Sensing,* **43,** 721-726.

Tucker, C.J., Vanpraet, C.L., Boerwinkel, E., and Gaston, A., 1983: Satellite remote sensing of total dry matter production in the Senegalese Sahel. *Remote Sens. Environ.,* **13,** 461-474.

Tucker, C.J., Vanapraet, C.L., Sharman, M.J., and Van Ittersum, G., 1985a: Satellite remote sensing of total herbaceous biomass production in the Senegalese Sahel: 1980-1984. *Remote Sens. Environ.,* **17,** 233-249.

Tucker, C.J., Townshend, J.R.G., and Goff, T.E., 1985b: African land-cover classification using satellite data. *Science,* **227,** 369-375.

Tucker, C.J., and Sellers, P.J., 1986: Satellite remote sensing of primary production. *Int. J. Remote Sens.,* **7,** 1395-1416.

Tucker, C.J., Newcomb, W.W., Los, S.O., and Prince, S.D., 1991: Mean and inter-year variation of growing-season normalized difference vegetation index for the Sahel 1981-1989. *Int. J. Remote Sens.,* **12,** 1133-1135.

White, F., 1983: *The Vegetation of Africa.* UNESCO, Paris, 383pp.

Vita

Captain Matthew R. Williams was born on January 2, 1964, in Oakland, California. He graduated from Winter Haven High School, Winter Haven, Florida, in 1982. He then attended Florida State University and was awarded a Bachelor of Science degree in Meteorology in April, 1986. He attended Officer Training School at Lackland Air Force Base, San Antonio, and received a Second Lieutenant's commission in the United States Air Force in October, 1986. From November, 1986, to March, 1989, he was a Wing Weather Officer at Cannon Air Force Base, New Mexico, followed by a fourteen month assignment to Osan Air Base, Republic of Korea, as a forecaster and Wing Weather Officer. In August of 1990, Captain Williams returned to Florida State University to begin his gradute studies.